This document contains the **post-print pdf-version** of the refereed paper:

"*An interactive decision-support system for multi-objective optimization of nonlinear dynamic processes with uncertainty.*"

by *Mattia Vallerio, Jan Hufkens, Jan Van Impe and Filip Logist*

which has been archived on the university repository Lirias (https://lirias.kuleuven.be/) of the KU Leuven.

The content is identical to the content of the published paper, but without the final typesetting by the publisher.

When referring to this work, please cite the full bibliographic info:

M. Vallerio, J. Hufkens, J. Van Impe and F. Logist (2015). An interactive decision-support system for multi-objective optimization of nonlinear dynamic processes with uncertainty. Expert Systems with Applications, 42 (21), 7710-7731.

The journal and the original published paper can be found at:
http://www.journals.elsevier.com/expert-systems-with-applications
http://www.sciencedirect.com/science/article/pii/S0957417415003747
doi:10.1016/j.eswa.2015.05.038

The corresponding author can be contacted for additional info.

Conditions for open access are available at:
http://www.sherpa.ac.uk/romeo/

Postprint version of paper published in Expert Systems with Applications 2015, vol. 42, p. 7710-7731.
The content is identical to the published paper, but without the final typesetting by the publisher.

An interactive decision-support system for multi-objective optimization of nonlinear dynamic processes with uncertainty

Mattia Vallerio[a], Jan Hufkens[a], Jan Van Impe[a], Filip Logist[a,*]

[a]*BioTeC+ & OPTEC, KU Leuven, Department of Chemical Engineering, W. de Croylaan 46, B-3001 Leuven, Belgium*

Abstract

The manufacturing industry is faced with the challenge to constantly improve its processes, e.g., due to lower profit margins, more strict environmental policies and increased societal awareness. These three aspects are considered as the pillars of *sustainable development* and typically give rise to multiple and conflicting objectives. Hence, any decision made will require trade-offs to be evaluated and compromises to be made. To support decision-making an interactive multi-objective framework is presented to optimize dynamic processes based on mathematical models. The framework includes a numerically efficient strategy to account for parametric uncertainty in the models and it allows to directly minimize the operational risks arising from this uncertainty. Hence, for the first time expert knowledge on the trade-offs between traditional objective functions and operational risks is readily and interactively available for the practitioners in the field of dynamic systems. The introduced interactive framework for multi-objective dynamic optimization under uncertainty is successfully tested for a three and five-objective fed-batch reactor case study with uncertain feed temperature and heat transfer parameters.

Keywords: multi-objective optimization, dynamic optimization, optimal control, robust optimization, nonlinear optimization, interactive tool

*Corresponding author
Email address: {mattia.vallerio,jan.vanimpe,filip.logist}@cit.kuleuven.be (Filip Logist)

Journal homepage: http://www.journals.elsevier.com/expert-systems-with-applications
Original file available at: http://www.sciencedirect.com/science/article/pii/S0957417415003747

Postprint version of paper published in Expert Systems with Applications 2015, vol. 42, p. 7710-7731.
The content is identical to the published paper, but without the final typesetting by the publisher.

1. Introduction

The increased awareness towards societal (e.g., increase safety and maintain/increase occupational level) and environmental aspects (e.g., decrease energy consumption and decrease emissions) of public institutions has indicated *sustainable development* as a main target for the whole global manufacturing industry. The priorities and targets of the EU growth strategy Europe-2020 confirmed this trend. An important aspect of *sustainable development* includes targeting a more *sustainable operation* of the existing technologies.

Dynamic mathematical models and model based optimization techniques have for more than 30 years contributed to improvements in economic sustainability (e.g., maximize profit or production) of industrial processes. However, much less effort has been spent on: (i) the inclusion of societal and environmental impact within optimization studies, (ii) the *trade-offs* arising between all objectives, (iii) the proposition of different optimal improvement alternatives (iv) the efficient visualization and analysis of proposed alternatives and (v) the making of well-informed decisions for operation under uncertainty.

1.1. Multi-objective and model based optimization as Expert Systems

For all these reasons, it is crucial to recognize the value of model based optimization and multi-objective optimization (MOO) algorithms as powerful *expert systems*. In particular, one should consider how difficult it would be for a human-being to decide upon tens of degrees of freedom, subjected to (possibly) non-linear dynamic equations, constraints and objective functions. Adding to this mix, multiple and conflicting objectives, uncertainty and multi-dimensional data, makes the task of selecting an optimal operation policy extremely daunting. Hence, there is the need to develop advanced *expert systems* that draw from several different research directions (e.g., multi-objective optimization, model based dynamic optimization, interactive software design, information theory,

Journal homepage: http://www.journals.elsevier.com/expert-systems-with-applications
Original file available at: http://www.sciencedirect.com/science/article/pii/S0957417415003747

Postprint version of paper published in Expert Systems with Applications 2015, vol. 42, p. 7710-7731.
The content is identical to the published paper, but without the final typesetting by the publisher.

decision-making and data visualization and analysis) to support experts in the field to make sound and reliable decisions in real-time.

With respect to multi-objective optimization, typically, a single solution that optimizes all conflicting objectives simultaneously is not possible, but there exists a set of mathematically equivalent solutions, known as the *Pareto set* (**?**). In order to select the best solution among this set of alternatives, an expert in the field of the investigated problem , i.e., a *decision-maker* (DM) is asked to express his/her preferences. To support decision-making in practice MOO can be exploited to help the DM generating different Pareto optimal alternatives according to his/her preferences and choosing among them. Based on the way these preferences are taken into account, it is possible to categorize the different MOO methods in (**?**): (i) *a priori*; the DM expresses his/her preferences before generating the solution, (ii) *a posteriori*; the DM decides based on a set of previously generated alternatives and (iii) *interactive*; the DM directly participates in the solution procedure by consecutively refining the set of generated solution according to his/her updated preferences.

1.2. Interactive multi-objective optimization

In the last decade the multi-objective optimization aspects in the operation of dynamic processes (resulting in so-called *multi-objective dynamic optimization* or *multi-objective optimal control problems* (MOOCPs)) have gained interest (see, e.g., **?????**). It has to be mentioned that these infinite dimensional optimal control problems are typically discretized resulting into finite dimensional large-scale nonlinear optimization problems (NLPs).

Hence, in this context it may become computationally expensive to compute a well-distributed set of Pareto points over the entire feasible criteria space or it might be a non-trivial task for the DM to correctly condense his/her preferences in mathematical terms. One possible solution comes from *interactive*

Journal homepage: http://www.journals.elsevier.com/expert-systems-with-applications
Original file available at: http://www.sciencedirect.com/science/article/pii/S0957417415003747

Postprint version of paper published in Expert Systems with Applications 2015, vol. 42, p. 7710-7731.
The content is identical to the published paper, but without the final typesetting by the publisher.

multi-objective optimization algorithms. These methods gradually explore the *Pareto set* based on a consecutive and repeated interaction with DM. During the human-algorithm interaction the DM can gain valuable knowledge about the problem and adjust his/her preferences according to constantly updated and refined information. Often, interactive methods implement an achievement scalarization function (ASF) (**?**) in one of its variants to generate Pareto optimal alternatives (**?**). As a consequence, it is possible to distinguish between methods according to the way the preference update is performed: (i) by updating the reference point (e.g., **????**) or by assigning the different objectives to categories, e.g., to be improved and can be worsened. An example of the latter class is the NIMBUS method (**?**). Recently, it has been extended to IND-NIMBUS with additional methods from the former class (**??**) and it was linked to the dynamic process simulator APROS (**?**).

The proposed interactive method differs from the previously mentioned approaches both from a theoretical and from a practical point of view. First of all, the proposed method is based on an interactive adaptation of the Normal Boundary Intersection (NBI, **?**) and Enhanced Normalized Normal Constraint (ENNC, **??**) methods. Hence, the DM does not express his/her preferences via a reference point or by assigning objectives to categories but via the *browsing* of the scalarization parameters, i.e., *weights*, space. This represents the first conceptual difference in respect to other interactive methods since there is a fundamental shift in paradigm during the interaction between the DM and the algorithm. A second difference is given by the active use of the Graphical User Interface (GUI) as a learning tool for the DM, when solving dynamic optimization problems. The proposed GUI allows the DM to grasp the underlying system dynamics and to identify possible process bottlenecks and critical constraints via the interactive visualization of the state and control profiles. After this first learning step the DM can decide either to refine the entire Pareto set or to add an additional point in a specific location of interest on the Pareto set. The use of the GUI to explore in depth the obtained dynamic optimization

Journal homepage: http://www.journals.elsevier.com/expert-systems-with-applications
Original file available at: http://www.sciencedirect.com/science/article/pii/S0957417415003747

Postprint version of paper published in Expert Systems with Applications 2015, vol. 42, p. 7710-7731.
The content is identical to the published paper, but without the final typesetting by the publisher.

solutions represents a novelty with respect to algorithm implementation which is necessary when dealing with dynamic systems. A similar approach to the one presented here was presented by **?**. There an interactive implementation of the Pascoletti-Serafini scalarization method (**?**, i.e., general case of NBI and ENNC) was used and it was connected to the steady-state flowsheet simulator CHEMASIM. Also there the DM updates his/her preferences by selecting the scalarization parameters via sliders. Additionally, in this work a sandwich approach (i.e., calculation of outer and inner approximations was used) to estimate the accuracy of the Pareto front. The main difference in methodology between the two methods is that in the proposed implementation a simplicial grid is imposed on the Pareto front, where the Pareto points are the vertices of the multi-dimensional simplices. This allows a better understanding of the relationship between points and it is also used to provide decision-support for problems with more than two objectives.

It has to be noted that all the interactive MOO methods discussed so far are based on deterministic scalarization methods, a separate discussion should be done for evolutionary strategies (e.g., **??**) and their interactive implementations (see, e.g., **??????????**). The reasons behind this is due to the differences between the way candidate Pareto solutions are generated and the fact that the DM interaction is mostly limited to the selection of a reference point. Hence, since the current work is based on deterministic and scalarization based approaches, for the sake of brevity, a detailed discussion on evolutionary based methods is not reported here.

Moreover, in order to exploit all the possible benefits and to limit the possible drawbacks coming from the deployment of human-algorithm interactions, a careful attention to the design of the interactivity features should be taken into account **?**. In this respect, it is crucial to avoid overloading the DM with too much information **??** which can undermine his/her decision capabilities, extend the time to reach a decision or even mislead him/her towards (possibly)

Journal homepage: http://www.journals.elsevier.com/expert-systems-with-applications
Original file available at: http://www.sciencedirect.com/science/article/pii/S0957417415003747

Postprint version of paper published in Expert Systems with Applications 2015, vol. 42, p. 7710-7731.
The content is identical to the published paper, but without the final typesetting by the publisher.

wrong search directions. A possible solution to this problem has been recently introduced by **?**. There, the DM is assisted by *agents*, which help guiding the exploration process towards predetermined search directions. Another possibility comes from a wider and more systematic use of concepts and tools (e.g., **?**) from the field of visual analytics (i.e., analytic reasoning supported by tailored data visualizations). In this respect the work of **?** can be considered a first starting point. In this work a step in this direction is done by allowing the DM to interactively select between different visualization methods both for the learning phase and for updating his/her preferences. In particular, for the latter case the proposed GUI makes use of dedicated decision-support windows that allow the DM to gain different insights and, therefore, build a stronger confidence in his/her decision in a shorter amount of time.

1.3. Quantify uncertainty to minimize operational risk

Additionally, another important contribution of the current work is the possibility to directly consider operational risks related to uncertainty in the process parameters as an objective function. Unfortunately, model based simulation and optimization are intrinsically affected by uncertainty in the model (e.g., **??**). When dealing with inherent parametric uncertainty, mainly two different strategies have been used in literature: (i) accounting for the states and/or parameters probability distribution by specifying *expected value optimization problems and chance constraints* (e.g., **??????**) or, (ii) formulating a *worst case scenario optimization* when the uncertainty is defined by a given set, e.g., a box or ellipsoid (see, e.g., **???** for optimal control and **?** for an online application). Other strategies to quantify and consider the system's variances are reported for example in **??**.

By directly accounting for uncertainty in optimization problems, an increased *robustness* for the obtained solution is achieved. For instance, chances that constraints are violated when the solution is applied, will be lower. However, this increased robustness is usually accompanied by a *performance loss*

Journal homepage: http://www.journals.elsevier.com/expert-systems-with-applications
Original file available at: http://www.sciencedirect.com/science/article/pii/S0957417415003747

Postprint version of paper published in Expert Systems with Applications 2015, vol. 42, p. 7710-7731.
The content is identical to the published paper, but without the final typesetting by the publisher.

(e.g., loss in productivity) in the process (**??**). Hence, *trade-offs* between robustness and performance are introduced and can be studied via MOO. It has to be emphasized that robust optimization problems typically require the addition of a significant number of equations to describe the uncertainty propagation and consequently are much larger in size and more complex than the original one.

Two frameworks for the solution of multi-objective problems under uncertainty have been proposed in **?** and **?**. However, the former is limited to scalar design optimization problems and the latter only reports bi-objective optimal control problem and it does not include interactive features. In this work the uncertainty is tackled in a computationally tractable way with a probabilistic approach via the Sigma Point (SP) method (**?**). Additionally, the operational risk related with the uncertainty is directly accounted as an additional objective function. This allows to directly quantify the trade-offs between more robust operating conditions and the other objectives.

1.4. Contribution

The current paper proposes a novel interactive adaptation of MOO scalarization algorithms (**????**) along with a tailored GUI for the evaluation of the *trade-offs* arising between multiple objectives in nonlinear *dynamic optimization* problems under uncertainty (so-called *robust multi-objective optimal control problems* (RMOOCPs)). The various contributions presented in this work are combined in the novel tool called *Pareto Browser* to be used for multi-objective dynamic optimization under uncertainty. The contribution can be summarized as follows:

1. **Development of an interactive multi-objective framework.** In contrast with existing interactive MOO methods, the proposed framework is based on the update of preferences by the DM via the selection of (weights) rather than indicating a reference point or categorizing the various objective functions. Additionally, the Pareto front is fitted with a

Journal homepage: http://www.journals.elsevier.com/expert-systems-with-applications
Original file available at: http://www.sciencedirect.com/science/article/pii/S0957417415003747

Postprint version of paper published in Expert Systems with Applications 2015, vol. 42, p. 7710-7731.
The content is identical to the published paper, but without the final typesetting by the publisher.

multi-dimensional simplicial grid. This grid allows for the definition of fast global, i.e., on the entire Pareto front, or local updating procedure for problems with more than two objectives. Moreover, the grid helps the DM understand the relationship between different points. Different visualization strategies (e.g., Parallel Coordinates and Level Diagrams) are deployed in the framework to allow the DM to gain different insights and, therefore, build a stronger confidence in his/her decision in a shorter amount of time.

2. **Minimization of operational risk.** A computationally tractable formulation is proposed, which considers parametric uncertainty and casts the operational risk as an additional objective function. Also constraint satisfaction in spite of related uncertainty is included. This allows to directly quantify the trade-offs arising when a robust solution is adopted.

3. **Direct visualization of dynamic profiles and related robustness.** The proposed framework allows the direct visualization of dynamic state and control profiles. Additionally, the robustness level associated with each profile is also depicted, allowing a direct quantification of the operational risk involved. This feature is tailor made for dynamic systems and it has been found necessary during the decision process.

4. **Efficient solution of large-scale NLPs.** The proposed framework can efficiently tackle the large-scale NLPs arising from the discretization of the multi-objective dynamic optimization problems under uncertainty. This enables the possibility to use the proposed framework as a real-time decision-making tool avoiding the need to postpone decisions due to lengthy solution times.

The article is structured as follows: First, Section 2 introduces the key elements for (i) multi-objective optimization, (ii) optimization under uncertainty, (iii) dynamic optimization and finally (iv) robust multi-objective optimal control, and formulates the relevant optimization problems mathematically. Then,

Journal homepage: http://www.journals.elsevier.com/expert-systems-with-applications
Original file available at: http://www.sciencedirect.com/science/article/pii/S0957417415003747

Postprint version of paper published in Expert Systems with Applications 2015, vol. 42, p. 7710-7731.
The content is identical to the published paper, but without the final typesetting by the publisher.

Section 3 illustrates the developed interactive *Pareto Browser* via the solution of a three-objective RMOOCP for a fed-batch reactor. Afterwards, Section 4 presents the application of the *Pareto Browser* for high-dimensional problems on a five-objective RMOOCP. Section 5 discusses the advantages and the drawbacks of the proposed framework and highlights future research lines for the field of interactive MOO as an expert system tool. Finally, Section 6 draws the conclusions on the presented work.

2. Mathematical formulation and methods

2.1. Multi-objective optimization

2.1.1. Formulation

A general multi-objective optimization problem[1] (MOOP) is formulated as follows:

$$\min_{\mathbf{y}\in\mathbb{R}^n} \{J_1(\mathbf{y}), J_2(\mathbf{y}), \ldots, J_{\mathrm{m}}(\mathbf{y})\} \tag{1}$$

$$\text{subject to :} \quad \mathbf{g}(\mathbf{y}) \geq \mathbf{0} \tag{2}$$

$$\mathbf{h}(\mathbf{y}) = \mathbf{0} \tag{3}$$

Here, $\mathbf{y}$ are all the optimization variables and the set of feasible solutions $\mathcal{S}$ is defined as all vectors $\mathbf{y}$ that satisfy the imposed constraints (2) and (3). The individual *objective functions* $J_{\mathrm{i}}(\mathbf{y})$ can be grouped into the *cost vector* $\mathbf{J}(\mathbf{y}) = [J_1(\mathbf{y}), J_2(\mathbf{y}), \ldots, J_{\mathrm{m}}(\mathbf{y})]^{\intercal}$. As optimality criterion, the concept of *Pareto optimality* is adopted.

Definition. A point $\mathbf{y}^* \in \mathcal{S}$, is Pareto optimal if and only if there does not exist another point $\mathbf{y} \in \mathcal{S}$, such that $J_{\mathrm{i}}(\mathbf{y}) \leq J_{\mathrm{i}}(\mathbf{y}^*)$ for all i and $J_{\mathrm{i}}(\mathbf{y}) < J_{\mathrm{i}}(\mathbf{y}^*)$

[1] Without loss of generality only scalar formulations are presented in view of brevity.

Journal homepage: http://www.journals.elsevier.com/expert-systems-with-applications
Original file available at: http://www.sciencedirect.com/science/article/pii/S0957417415003747

Postprint version of paper published in Expert Systems with Applications 2015, vol. 42, p. 7710-7731.
The content is identical to the published paper, but without the final typesetting by the publisher.

for at least one objective function.

Furthermore, the following items are introduced: the *minimizer* $\mathbf{y}_\mathrm{i}^*$ of the i-th cost function $J_\mathrm{i}(\mathbf{y})$, the *utopia point* $\mathbf{J}^* = [J_1^*, J_2^*, \ldots, J_\mathrm{m}^*]^\intercal$ which contains the minima of the individual objective functions $J_\mathrm{i}(\mathbf{y}_i^*)$, the *individual minima* cost vectors or *anchor points* $\mathbf{J}(\mathbf{y}_\mathrm{i}^*)$, which is the cost vector evaluated for the individual minimizer $\mathbf{y}_\mathrm{i}^*$, the *pay-off* matrix $\mathbf{\Phi}$, whose i-th column is $\mathbf{J}(\mathbf{y}_\mathrm{i}^*) - \mathbf{J}^*$. The *Convex Hull of Individual Minima* CHIM is defined as the set of points in $\mathbb{R}^\mathrm{m}$ that are a convex combination of $\mathbf{J}(\mathbf{y}_\mathrm{i}^*)$ - $\mathbf{J}^*$, i.e., $\{\mathbf{\Phi w} \ : \ \mathbf{w} \in \mathbb{R}^\mathrm{m} \ , \sum_{\mathrm{i}=1}^\mathrm{m} w_\mathrm{i}, w_\mathrm{i} \geq 0\}$.

2.1.2. Multi-objective scalarization methods

Scalarization methods reformulate the MOOP into a parametric single-objective optimization problem (SOOP). By consistently varying the scalarization parameters (often called *weights* $\mathbf{w}$) an approximation of the Pareto set is obtained. However, the computation of the entire set can become expensive. Moreover, most often the DM is only interested in a specific part of the Pareto front. Hence, it is interesting to exploit the algorithms in an interactive way.

Weighted Sum (WS). The convex Weighted Sum is still often used in practice:

$$\min_{\mathbf{y} \in \mathbb{R}^n} J_\mathrm{WS} = \sum_{\mathrm{i}=1}^\mathrm{m} w_\mathrm{i} J_\mathrm{i}(\mathbf{y}) \tag{4}$$

$$\tag{5}$$

$$\text{subject to :} \quad \mathbf{g}(\mathbf{y}) \geq \mathbf{0} \tag{6}$$

$$\mathbf{h}(\mathbf{y}) = \mathbf{0} \tag{7}$$

Journal homepage: http://www.journals.elsevier.com/expert-systems-with-applications
Original file available at: http://www.sciencedirect.com/science/article/pii/S0957417415003747

Postprint version of paper published in Expert Systems with Applications 2015, vol. 42, p. 7710-7731.
The content is identical to the published paper, but without the final typesetting by the publisher.

with $w_i \geq 0$ and $\sum_{i=1}^{m} w_i = 1$. The WS has several intrinsic drawbacks **?**. Non-convex parts of the Pareto set cannot be explored and an even distribution of weights does not necessarily lead to a uniform discretization of the Pareto set.

Normal Boundary Intersection (NBI). NBI is a specific case of the Pascoletti-Serafini method **?** and reformulates the MOOP as follows **?**:

$$\max_{\mathbf{y}\in\mathbb{R}^n,\ t_{\mathrm{NBI}}\in\mathbb{R}} t_{\mathrm{NBI}}, \tag{8}$$

$$\text{subject to :} \quad \mathbf{g}(\mathbf{y}) \geq \mathbf{0} \tag{9}$$

$$\mathbf{h}(\mathbf{y}) = \mathbf{0} \tag{10}$$

$$\mathbf{\Phi w} - \lambda \mathbf{\Phi e} = \mathbf{J}(\mathbf{y}) - \mathbf{J}^* \tag{11}$$

with weights $w_i \geq 0$, $\sum_{i=1}^{m} w_i = 1$ and $\mathbf{e} = [1, 1, ..., 1]^\intercal \in \mathbb{R}^m$ the m-dimensional vector containing all ones. Hence, $\mathbf{\Phi w}$ indicates a point on the CHIM, and $-t_{\mathrm{NBI}}\mathbf{\Phi e}$ describes the (quasi-)normal direction to the CHIM. The rationale is that the intersection between the (quasi-)normal from any point $\mathbf{\Phi w}$ and the boundary of the feasible cost space closest to the utopia point is expected to be Pareto optimal. To this end, Eq. (8) introduces the maximization of the length t_{NBI} along the (quasi-)normal described by m additional equality constraints (Eq. (11)). NBI has been reported to mitigate the intrinsic drawbacks of the WS mentioned above **?**. A geometric interpretation of NBI and analytic relations linking an NBI solution to the corresponding WS solution can be found in **?**.

(Enhanced) Normalized Normal Constraint ((E)NNC).. ENNC reformulates the original MOO in an alternative way **??**:

$$\min_{\mathbf{y}\in\mathbb{R}^n} \hat{J}_m, \tag{12}$$

$$\tag{13}$$

Journal homepage: http://www.journals.elsevier.com/expert-systems-with-applications
Original file available at: http://www.sciencedirect.com/science/article/pii/S0957417415003747

Postprint version of paper published in Expert Systems with Applications 2015, vol. 42, p. 7710-7731.
The content is identical to the published paper, but without the final typesetting by the publisher.

$$\text{subject to}: \quad \mathbf{g}(\mathbf{y}) \geq \mathbf{0} \tag{14}$$

$$\mathbf{h}(\mathbf{y}) = \mathbf{0} \tag{15}$$

$$(\hat{\mathbf{J}}(\mathbf{y}^*_{\mathrm{m}}) - \hat{\mathbf{J}}(\mathbf{y}^*_{\mathrm{i}}))^{\intercal}(\hat{\mathbf{\Phi}}\mathbf{w} - \hat{\mathbf{J}}(\mathbf{y})) \geq \mathbf{0} \text{ for } \mathrm{i} = 1, \ldots, \mathrm{m}-1, \tag{16}$$

where $\hat{}$ indicates variables based on *normalized* objectives. The rationale is to minimize the a single objective (Eq. (12)), while reducing the feasible cost space by adding $\mathrm{m}-1$ hyperplanes given by Eq. (16) that are orthogonal to the CHIM. Normalization is achieved as proposed in **?**. Analytic relations linking solutions of ENNC to NBI can be found in **?**.

2.2. Robust optimization

2.2.1. Formulation

Generally, a scalar optimization problem subject to uncertain parameters can be formulated as follows[2]:

$$\min_{\mathbf{y} \in \mathbb{R}^n} J(\mathbf{y}, \boldsymbol{\lambda}), \tag{17}$$

$$\text{subject to}: \quad \mathbf{g}(\mathbf{y}, \boldsymbol{\lambda}) \geq \mathbf{0}, \tag{18}$$

$$\mathbf{h}(\mathbf{y}, \boldsymbol{\lambda}) = \mathbf{0}. \tag{19}$$

with n_λ the number of uncertain parameters in the vector $\boldsymbol{\lambda}$. In the current paper, these parameters are assumed to be determined by a probability distribution. Hence, in order to convert the above optimization problem into a formulation with *expected values* and single *chance constraints* a technique to propagate the uncertainty is needed.

[2] Again a scalar formulation is presented for reasons of brevity.

Journal homepage: http://www.journals.elsevier.com/expert-systems-with-applications
Original file available at: http://www.sciencedirect.com/science/article/pii/S0957417415003747

Postprint version of paper published in Expert Systems with Applications 2015, vol. 42, p. 7710-7731.
The content is identical to the published paper, but without the final typesetting by the publisher.

2.2.2. Uncertainty propagation using the Sigma Point method

The Sigma Point (SP) method allows to efficiently approximate probability distributions mapped through nonlinear transformations. The method was proposed in **?** and it is centered on the intuitive notion of approximating a distribution via a fixed number of points in the parameter space (i.e., the so-called *Sigma Points*), rather than approximating an arbitrary nonlinear function. Figure 1 illustrates the principles of the Sigma Point method applied to a function with two uncertain parameters. The dots on the oval represent the four new parameter values for which the nonlinear function has to be additionally evaluated. The propagation of the nominal parameter value and the four newly introduced parameter values through the nonlinear function gives rise to five outputs in total. These outputs are then used to compute the *expected value* and *variance-covariance*. This transformation can be, in a model-based optimization framework, regarded as the simulation of the process model and/or the evaluation of the objective function(s) and constraints.

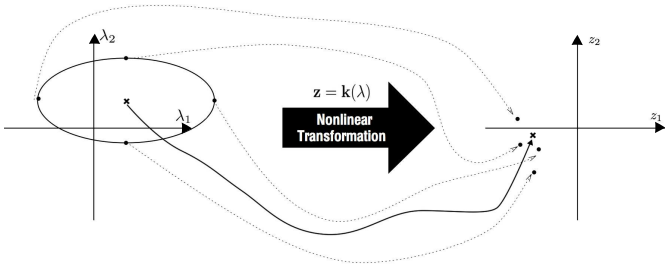

Figure 1: Illustration of the sigma point method. On the left, the parameter space is displayed. The four dots on the oval represent the four parameter variations. These four variations as well as the expected parameter values (the center of the oval) are propagated through the nonlinear transformation $\mathbf{k}$. Based on the obtained results the expected value and variance-covariance can be approximated.

Mathematically, this can be expressed as follows. Assume the following nonlinear function:

$$\mathbf{z} = \mathbf{k}(\boldsymbol{\lambda}) \ , \tag{20}$$

Journal homepage: http://www.journals.elsevier.com/expert-systems-with-applications
Original file available at: http://www.sciencedirect.com/science/article/pii/S0957417415003747

Postprint version of paper published in Expert Systems with Applications 2015, vol. 42, p. 7710-7731.
The content is identical to the published paper, but without the final typesetting by the publisher.

where the vector $\boldsymbol{\lambda}$ has a specific distribution with a given expected value $\bar{\boldsymbol{\lambda}}$ and *variance-covariance* matrix $\mathbf{P}_\lambda$. The sigma points are defined as:

$$\pi_0 = \bar{\boldsymbol{\lambda}}, \tag{21}$$

$$\pi_\mathrm{i} = \bar{\boldsymbol{\lambda}} + \sqrt{(\mathrm{n}_\lambda + \kappa)\mathrm{P}_{\lambda_\mathrm{i}}} \quad \text{with i} = 1, \ldots, \mathrm{n}_\lambda, \tag{22}$$

$$\pi_\mathrm{i} = \bar{\boldsymbol{\lambda}} - \sqrt{(\mathrm{n}_\lambda + \kappa)\mathrm{P}_{\lambda_{\mathrm{i}-\mathrm{n}_\lambda}}}, \quad \text{with i} = \mathrm{n}_\lambda + 1, \ldots, 2\mathrm{n}_\lambda \tag{23}$$

A total of $2\mathrm{n}_\lambda + 1$ Sigma Points is needed, where n_λ is the dimension of the vector $\boldsymbol{\lambda}$. $\sqrt{\mathbf{P}_{\lambda_\mathrm{i}}}$, denotes the i-th column of the matrix square root, which can be computed by, e.g., a Cholesky decomposition. These Sigma Points are then evaluated via the nonlinear function:

$$\zeta_\mathrm{i} = \mathbf{k}(\pi_\mathrm{i}) \quad \text{with i} = 0, \ldots, 2\mathrm{n}_\lambda. \tag{24}$$

The mean can be approximated as:

$$\bar{\mathbf{z}} = \frac{1}{\mathrm{n}_\lambda + \kappa} \left(\kappa\zeta_0 + \frac{1}{2} \sum_{i=1}^{2\mathrm{n}_\lambda} \zeta_\mathrm{i} \right) , \tag{25}$$

while the *variance-covariance* matrix is approximated as:

$$\mathbf{P}_{zz} = \frac{1}{\mathrm{n}_\lambda + \kappa} (\kappa(\zeta_0 - \bar{\mathbf{z}})(\zeta_0 - \bar{\mathbf{z}})^\top + \frac{1}{2} \sum_{\mathrm{i}=1}^{2\mathrm{n}_\lambda} (\zeta_\mathrm{i} - \bar{\mathbf{z}})(\zeta_\mathrm{i} - \bar{\mathbf{z}})^\top). \tag{26}$$

An answer to the question how to choose the parameter κ and a thorough theoretical analysis of the approximation errors can be found in **?**. Note also that the choice of these Sigma Points is not unique. Several methods, each with their advantages have been proposed in **?**. However, in the current study κ is taken equal to $3 - \mathrm{n}_\lambda$.

2.2.3. Sigma point formulation for robust optimization

In this section the extension of the SP method for optimization problems under uncertainty is described.

Journal homepage: http://www.journals.elsevier.com/expert-systems-with-applications
Original file available at: http://www.sciencedirect.com/science/article/pii/S0957417415003747

Postprint version of paper published in Expert Systems with Applications 2015, vol. 42, p. 7710-7731.
The content is identical to the published paper, but without the final typesetting by the publisher.

The nonlinear map $\mathbf{k}(\boldsymbol{\lambda})$ in Eq. (20) relates in an optimization context to the evaluation of the objective function $J(\mathbf{y}, \boldsymbol{\lambda})$ for given decision variables $\mathbf{y}$ that satisfy the equality constraints $\mathbf{h}(\mathbf{y}, \boldsymbol{\lambda}) = 0$. Hence, the objective function $J(\mathbf{y}, \boldsymbol{\lambda})$ has to be evaluated $2\mathrm{n}_\lambda + 1$ times in order to approximate its *expected value* $\bar{J}(\mathbf{y})$ as:

$$\bar{J}(\mathbf{y}) = \frac{1}{\mathrm{n}_\lambda + \kappa} \left(\kappa J(\mathbf{y}, \pi_0) + \frac{1}{2} \sum_{\mathrm{i}=1}^{2\mathrm{n}_\lambda} J(\mathbf{y}, \pi_\mathrm{i}) \right). \tag{27}$$

Also the objective function's *variance* $\mathbf{P}_\mathrm{J}$ can be approximated with negligible additional computational effort in analogy with Eqs. (25) and (26).

Similarly, the SP method allows for the computation of the *expected constraint values*, $\bar{\mathbf{g}}(\mathbf{y}, \boldsymbol{\lambda})$, and the associated *variance-covariance* matrices $\mathbf{P}_\mathrm{g}(\mathbf{y}, \boldsymbol{\lambda})$ with negligible additional computational effort (see Eqs. (25) and (26)).

Consequently, a *robust optimization problem* with respect to uncertain parameters can be formulated as follows:

$$\min_{\mathbf{y} \in \mathbb{R}^n} \bar{J}(\mathbf{y}, \boldsymbol{\lambda}) + \alpha_\mathrm{J} \sqrt{P_\mathrm{J}(\mathbf{y}, \boldsymbol{\lambda})}, \tag{28}$$

$$\text{subject to :} \quad \mathbf{g}(\mathbf{y}, \pi_\mathrm{i}) \geq \mathbf{0} \text{ for } \mathrm{i} = 1, 2, \ldots, \mathrm{n}_\lambda \tag{29}$$

$$\mathbf{h}(\mathbf{y}, \pi_\mathrm{i}) = \mathbf{0} \tag{30}$$

$$\bar{\mathbf{g}}_\mathrm{j}(\mathbf{y}, \boldsymbol{\lambda}) - \alpha_{\mathrm{g,j}} \sqrt{\mathbf{P}_{\mathrm{g,jj}}}(\mathbf{y}, \boldsymbol{\lambda}) \geq \mathbf{0} \text{ for } \mathrm{j} = 1, 2, \ldots, \mathrm{n}_\mathrm{g} \tag{31}$$

Here, the scalar α_J and the vector α_g are *multiplication factors* that introduce a *performance loss* and a *constraint back-off*. It has to be noted that a first robustification effect comes from the requirement that all constraints have to be simultaneously satisfied for all *Sigma Points* (Eqs. (29)). A more relaxed approach could consist in requiring only the resulting *Expected value* of the constraints to be satisfied, and therefore leave the *Sigma Point* realizations

Journal homepage: http://www.journals.elsevier.com/expert-systems-with-applications
Original file available at: http://www.sciencedirect.com/science/article/pii/S0957417415003747

Postprint version of paper published in Expert Systems with Applications 2015, vol. 42, p. 7710-7731.
The content is identical to the published paper, but without the final typesetting by the publisher.

free to violate the constraints. A second robustifaction effect is added with the introduction of the *variance-covariance* matrix $\mathbf{P}_{\mathrm{g}}$ in the constraint formulation (Eq. (31)). This equation can be interpreted as a series of probabilistic single *chance constraints* (i.e., one for each constraint g_{j} in the vector $\mathbf{g}$) with $\mathbf{P}_{\mathrm{g,jj}}$ the j-th diagonal element of the *variance-covariance* matrix $\mathbf{P}_{\mathrm{g}}$ related to the j-th constraint g_{j}:

$$Pr(\bar{\mathbf{g}}_j(\mathbf{y}, \boldsymbol{\lambda}) - \alpha_{\mathrm{g_j}} \sqrt{\mathbf{P}_{\mathrm{g,jj}}} \geq \mathbf{0}) \leq A \tag{32}$$

which requires that the probability of violation is less than $(100 - A)\%$. The interesting aspect is that the level of confidence, i.e., the value of A can be manipulated through the multiplication factor α_{g}. Moreover, if the probability density function of the constraints can be assumed to be normal then the multiplication factors α_{g} have the straightforward interpretation of quantiles of the Gaussian distribution. Hence, if for example $\alpha_{\mathrm{g}} = 1.96$ in Eq. (32), then A corresponds to a 95% probability. In other words, the single chance constraint has to be satisfied in 95% of the realizations. It has to be stressed that the assumption of (approximate) normality on the probability density function of the constraints can and has to be checked afterwards, e.g., via Monte Carlo simulations. If a too high percentage of violations is observed, the multiplication factor can be adjusted. Including these Monte-Carlo simulations, however, in the optimization itself will in general be computationally too expensive.

However, a dedicated loop to adjust the value of α_{g} can be implemented. Additionally, if the resulting uncertainty distribution appears not to be normal, but, e.g. multi-modal, a different procedure for the generation of the *sigma points* specifically tailored to tackle this kind of distribution should be adopted (**?**). Finally, if the resulting uncertainty distribution would present discontinuities or not fall back in a well-known category. A more detailed investigation of the dependency of the model from the considered uncertain parameters should be carried out.

Journal homepage: http://www.journals.elsevier.com/expert-systems-with-applications
Original file available at: http://www.sciencedirect.com/science/article/pii/S0957417415003747

Postprint version of paper published in Expert Systems with Applications 2015, vol. 42, p. 7710-7731.
The content is identical to the published paper, but without the final typesetting by the publisher.

Table 1: Chances and frequencies for a normally distributed event to be outside the confidence region, assuming that the event happens once a day.

α_g	Chance outside CR [%]	Occurence: once every ...
1	3.2×10^{1}	3 days
2	4.6	22 days
3	2.7×10^{-1}	1 year
4	6.3×10^{-3}	43 years
5	5.7×10^{-5}	4779 years
6	2.0×10^{-7}	1.4 million (10^6) years
7	2.6×10^{-10}	1.1 billion (10^9) years
8	1.2×10^{-13}	2.2 trillion (10^{12}) years

In the current work the values of the parameter α_g will not be assigned a priori but will be regarded as additional objective functions. This allows to directly quantify the *trade-offs* arising between increasing robustness and decreasing performance. However, no additional penalty related to the objective function's variance is imposed on the the objective (i.e., α_J equals zero.) As an illustration, Table 1 gives an idea of the frequency of occurrence for different values of α_g. It is clear that a deviation of 8σ is an extraordinary situation. On the other hand, a *confidence region* (CR) with only 1σ or 2σ is very likely to be exceeded. Consequently, the higher the value of α_g, the more confident the DM can be that the investigated system will not exceed the corresponding constraint, leading to a direct reduction of the operational risk.

2.3. Dynamic optimization or optimal control

2.3.1. Formulation

In dynamic optimization or optimal control, dynamic processes described by differential equations are optimized:

$$\min_{\mathbf{x}(\xi),\mathbf{u}(\xi),\xi_f} J(\mathbf{x}(\xi),\mathbf{u}(\xi),\xi_f,\mathbf{p}) = h(\mathbf{x}(\xi_f),\mathbf{p},\xi_f) + \int_0^{\xi_f} g(\mathbf{x}(\xi),\mathbf{u}(\xi),\mathbf{p},\xi)d\xi. \quad (33)$$

Journal homepage: http://www.journals.elsevier.com/expert-systems-with-applications
Original file available at: http://www.sciencedirect.com/science/article/pii/S0957417415003747

Postprint version of paper published in Expert Systems with Applications 2015, vol. 42, p. 7710-7731.
The content is identical to the published paper, but without the final typesetting by the publisher.

$$\text{subject to :} \quad \frac{d\mathbf{x}}{d\xi} = \mathbf{f}(\mathbf{x}(\xi), \mathbf{u}(\xi), \xi, \mathbf{p}) \quad \xi \in [0, \xi_\mathrm{f}], \tag{34}$$

$$\mathbf{0} = \mathbf{b}_\mathrm{c}(\mathbf{x}(0), \mathbf{p}), \tag{35}$$

$$\mathbf{0} \geq \mathbf{c}_\mathrm{p}(\mathbf{x}(\xi), \mathbf{u}(\xi), \xi, \mathbf{p}), \tag{36}$$

$$\mathbf{0} \geq \mathbf{c}_\mathrm{t}(\mathbf{x}(\xi_\mathrm{f}), \xi_\mathrm{f}, \mathbf{p}), \tag{37}$$

Here, $\mathbf{x}$ are the state variables, while $\mathbf{u}$ and $\mathbf{p}$ denote the time-varying and time-constant control variables, respectively. The vector $\mathbf{f}$ represents the dynamic system equations (on the interval $\xi \in [0, \xi_\mathrm{f}]$) with initial conditions given by the vector $\mathbf{b}_\mathrm{c}$. In the current case $\mathbf{f}$ comprises Ordinary Differential Equations (ODEs), but extensions to Differential Algebraic Equations (DAEs) (e.g., **?**) as well as Partial Differential Equations (PDEs) are possible (e.g., **?**). The vectors $\mathbf{c}_\mathrm{p}$ and $\mathbf{c}_\mathrm{t}$ indicate, respectively, path and terminal inequality constraints on the states and controls. The objective function $J(\mathbf{x}, \mathbf{u}, \mathbf{p}, \xi_\mathrm{f})$ can consist of both terminal and integral terms, accounting for values at the interval end or along the entire interval, respectively.

2.3.2. Numerical methods

Two main classes of methods exist to solve optimal control problems: (i) *direct* and (ii) *indirect methods*. *Direct* methods are also known as *"first discretize, than optimize"* in contrast with *indirect* methods which follow the route *"first optimize, than discretize¨*. *Indirect* methods are based on the first-order necessary conditions for optimality and reformulate the optimal control problems in *two point boundary value problems* **?**. *Direct* methods convert the optimal control problem into a *nonlinear programming problem* (NLP). The NLP is then solved via, e.g., *sequential quadratic programming* approaches (SQP) or *interior point* methods (IP). These methods have become the most common approaches during the last decades. In particular, in this work the *orthogonal collocation* (OCol) is exploited **?**. Other *direct* methods, such as single and multiple shooting **?**, require the use of integrators to solve the system of dynamic equations. Instead, OCol fully discretizes the states, via third or higher-order (orthogonal)

Journal homepage: http://www.journals.elsevier.com/expert-systems-with-applications
Original file available at: http://www.sciencedirect.com/science/article/pii/S0957417415003747

Postprint version of paper published in Expert Systems with Applications 2015, vol. 42, p. 7710-7731.
The content is identical to the published paper, but without the final typesetting by the publisher.

polynomials, as well as the controls via a piecewise constant discretization. The obtained set of discretized variables is taken as the set of optimization variables in an NLP. The size of the NLPs arising with this problem is quite large, however, the NLPs usually exhibit a considerable level of structure and sparsity. Thus, dedicated algorithms, that exploit the problem structure become a necessity to efficiently solve the discretized problems.

2.4. Robust multi-objective optimal control

2.4.1. Formulation

In this section the information on robust optimization, multi-objective optimization and optimal control is combined leading to the following robust multi-objective optimal control problem formulation:

$$\min_{\mathbf{x}_\mathrm{i}(\xi),\mathbf{u}(\xi),\xi_\mathrm{f}} \left\{ \bar{J}_1, \bar{J}_2, \dots \bar{J}_\mathrm{m}, -\alpha_{\mathrm{c_p}}, -\alpha_{\mathrm{c_t}} \right\} \tag{38}$$

subject to:

$$\frac{d\mathbf{x}_\mathrm{i}}{d\xi} = \mathbf{f}(\mathbf{x}_\mathrm{i}(\xi), \mathbf{u}(\xi), \xi, \mathbf{p}, \pi_\mathrm{i}) \quad \xi \in [0, \xi_\mathrm{f}], \qquad \text{with } \mathrm{i} = 0, \dots, 2\mathrm{n}_\lambda, \tag{39}$$

$$\mathbf{0} = \mathbf{b}_\mathrm{c}(\mathbf{x}_\mathrm{i}(0), \mathbf{p}, \pi_\mathrm{i}), \tag{40}$$

$$\mathbf{0} \geq \mathbf{c}_\mathrm{p}(\mathbf{x}_\mathrm{i}(\xi), \mathbf{u}(\xi), \xi, \mathbf{p}, \pi_\mathrm{i}), \tag{41}$$

$$\mathbf{0} \geq \mathbf{c}_\mathrm{t}(\mathbf{x}_\mathrm{i}(\xi_\mathrm{f}), \xi_\mathrm{f}, \mathbf{p}, \pi_\mathrm{i}), \tag{42}$$

$$\mathbf{P}_{\mathrm{c_p}} = \frac{\kappa}{\mathrm{n}_\lambda + \kappa} \left((\mathbf{c}_{\mathrm{p},0} - \bar{\mathbf{c}}_\mathrm{p})(\mathbf{c}_{\mathrm{p},0} - \bar{\mathbf{c}}_\mathrm{p})^\top + \frac{1}{2} \sum_{i=1}^{2\mathrm{n}_\lambda} (\mathbf{c}_{\mathrm{p,i}} - \bar{\mathbf{c}}_\mathrm{p})(\mathbf{c}_{\mathrm{p,i}} - \bar{\mathbf{c}}_\mathrm{p})^\top \right), \tag{43}$$

$$\mathbf{P}_{\mathrm{c_t}} = \frac{\kappa}{\mathrm{n}_\lambda + \kappa} \left((\mathbf{c}_{\mathrm{t},0} - \bar{\mathbf{c}}_\mathrm{t})(\mathbf{c}_{\mathrm{t},0} - \bar{\mathbf{c}}_\mathrm{t})^\top + \frac{1}{2} \sum_{i=1}^{2\mathrm{n}_\lambda} (\mathbf{c}_{\mathrm{t,i}} - \bar{\mathbf{c}}_\mathrm{t})(\mathbf{c}_{\mathrm{t,i}} - \bar{\mathbf{c}}_\mathrm{t})^\top \right), \tag{44}$$

$$\mathbf{0} \geq \bar{\mathbf{c}}_{\mathrm{p,j}} + \alpha_{\mathrm{c_p}} \sqrt{\mathbf{P}_{\mathrm{c_p,jj}}} \qquad \text{for } \mathrm{j} = 1, \dots, \mathrm{n}_{\mathrm{c_p}} \tag{45}$$

$$\mathbf{0} \geq \bar{\mathbf{c}}_{\mathrm{t,j}} + \alpha_{\mathrm{c_t}} \sqrt{\mathbf{P}_{\mathrm{c_t,jj}}} \qquad \text{for } \mathrm{j} = 1, \dots, \mathrm{n}_{\mathrm{c_t}}. \tag{46}$$

The uncertainty is related to n_λ uncertain parameters $\boldsymbol{\lambda}$ with mean $\bar{\boldsymbol{\lambda}}$,

Journal homepage: http://www.journals.elsevier.com/expert-systems-with-applications
Original file available at: http://www.sciencedirect.com/science/article/pii/S0957417415003747

Postprint version of paper published in Expert Systems with Applications 2015, vol. 42, p. 7710-7731.
The content is identical to the published paper, but without the final typesetting by the publisher.

variance-covariance matrix $\mathbf{P}_\lambda$ and corresponding *Sigma Points* π_i. As a consequence, (i) expected values for all objective functions will be computed (Eq. (38)), (ii) path and terminal constraints will be required to be feasible for all *Sigma Points* (Eqs. (41) and (42)) and (iii) *chance constraints* will be imposed (Eqs. (45) and (46)). It has to be noted that the multiplication factors for *back-off* ($\alpha_{\mathrm{c_p}}$ and $\alpha_{\mathrm{c_t}}$) are regarded as additional objectives. However, as a minimization framework is presented here, a minus sign has to be placed in front of $\alpha_{\mathrm{c_p}}$ and $\alpha_{\mathrm{c_t}}$ to ensure for their maximization.

2.4.2. Developed framework

The framework that has been developed within the programming language Python integrates the methods detailed above. Figure 2 illustrates the framework schematically. As multi-objective optimization techniques, the weighted sum (WS), normal boundary intersection (NBI) and enhanced normalized normal constraint (ENNC) methods have been adopted. The scalarization parameter values or weights are initially generated automatically to enable a first exploration of the criterion space, while afterwards they can be adapted interactively. The exact interaction features and graphical user interface that have been added will be illustrated in the next section based on a case study. To enable a computationally tractable uncertainty propagation through the optimization problem the Sigma Point method is exploited. To tackle the optimal control problem a direct orthogonal collocation approach is employed which results in a large-scale NLP that is solved using the interior point optimizer IPOPT **?**. To speed up convergence exact derivative information (i.e., gradients, jacobians and hessian) is provided through efficient automatic differentiation techniques **?**. Although the presented framework is focussed on optimal control problems, it has to be stressed that any model-based optimization problem with multiple objectives can be tackled as long as it can be described as an NLP.

Journal homepage: http://www.journals.elsevier.com/expert-systems-with-applications
Original file available at: http://www.sciencedirect.com/science/article/pii/S0957417415003747

Postprint version of paper published in Expert Systems with Applications 2015, vol. 42, p. 7710-7731.
The content is identical to the published paper, but without the final typesetting by the publisher.

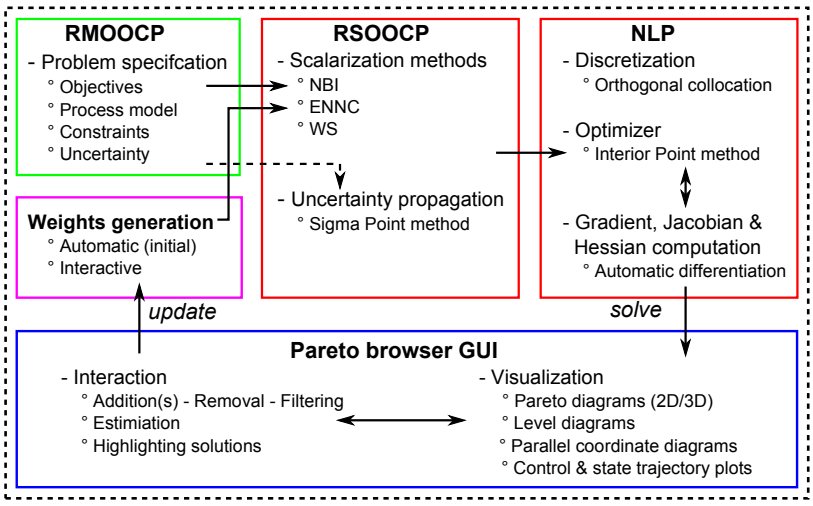

Figure 2: *Pareto Browser*'s schematic overview.

3. Interactive NBI/ENNC algorithms and Pareto Browser GUI

In this section an interactive adaptation of the NBI and ENNC algorithms (see Section 2.1.2) is introduced. The algorithm is coupled with a tailored Graphical User Interface (GUI) to exploit all the capabilities of the proposed interactive algorithm. The combination of the interactive algorithm and the GUI is referred to as *Pareto Browser*. The *Pareto Browser* not only allows an interactive solution of robust multi-objective optimal control problems (RMOOCPs) but it also features different interactive visualization methods to further enhance the understanding of the obtained solutions and help the decision-maker express his/her preferences.

3.1. Interactive adaptation of NBI and ENNC methods

Both NBI and ENNC are based on the calculation of the *individual minima* cost vectors or anchor points $\mathbf{J}(\mathbf{y}_i^*)$ to define the CHIM. Typically, once the CHIM is defined, it is then evenly discretized with a set of scalarization parameter vectors. Each of these vectors is then used to formulate a single-objective

Journal homepage: http://www.journals.elsevier.com/expert-systems-with-applications
Original file available at: http://www.sciencedirect.com/science/article/pii/S0957417415003747

Postprint version of paper published in Expert Systems with Applications 2015, vol. 42, p. 7710-7731.
The content is identical to the published paper, but without the final typesetting by the publisher.

optimization problem (SOOP).

The interactive versions iNBI and iENNC presented here are based on the interactive use of the scalarization parameters space to *browse* the *Pareto set*. In particular, the CHIM is a projection of the weight space, obtained when the anchor points are solved. Hence, the idea behind the proposed algorithm is to avoid the complete discretization of the CHIM but rather use it as a map to browse the subtended *Pareto set* by interactively defining one or more scalarization parameter vectors at a time.

Additionally, to guide the DM through the browsing of the *Pareto set* for three-dimensional problems, each Pareto point added to the set is organized based on a simplicial (i.e., triangular for 3D) scheme. In other words, simplices/triangles are formed between points obtained on the front. The shape of the triangles is automatically updated when a new point is added or a point is removed from the *Pareto set*.

3.2. Case study: A fed-batch reactor with uncertain parameters

The Williams-Otto fed-batch reactor is considered. The following reaction scheme takes place in the reactor: $A+B \rightarrow C$, $C+B \rightarrow P+E$ and $P+C \rightarrow G$. From these compounds, A is initially present in the reactor and B is fed. The products P and E are useful products, whereas product G is an undesired by-product. All the model parameters, their values, the initial conditions and additional constraints are reported in literature **??**.

Reactor model. The reactor model can be expressed as follows:

Journal homepage: http://www.journals.elsevier.com/expert-systems-with-applications
Original file available at: http://www.sciencedirect.com/science/article/pii/S0957417415003747

Postprint version of paper published in Expert Systems with Applications 2015, vol. 42, p. 7710-7731.
The content is identical to the published paper, but without the final typesetting by the publisher.

$$\frac{\mathrm{d}}{\mathrm{d}t}x_A(t) = -\frac{x_A u_1}{1000V} - k_1\eta_1 x_A x_B, \tag{47}$$

$$\frac{\mathrm{d}}{\mathrm{d}t}x_B(t) = \frac{(1-x_B)u_1}{1000V} - k_1\eta_1 x_A x_B - k_2\eta_2 x_B x_C, \tag{48}$$

$$\frac{\mathrm{d}}{\mathrm{d}t}x_C(t) = -\frac{x_C u_1}{1000V} + k_7\eta_1 x_A x_B - k_3\eta_2 x_B x_C - k_6\eta_3 x_C x_P, \tag{49}$$

$$\frac{\mathrm{d}}{\mathrm{d}t}x_P(t) = -\frac{x_P u_1}{1000V} + k_2\eta_2 x_B x_C - k_4\eta_3 x_C x_P, \tag{50}$$

$$\frac{\mathrm{d}}{\mathrm{d}t}x_E(t) = -\frac{x_E u_1}{1000V} + k_3\eta_2 x_B x_C, \tag{51}$$

$$\frac{\mathrm{d}}{\mathrm{d}t}x_G(t) = -\frac{x_G u_1}{1000V} - k_5\eta_3 x_C x_P, \tag{52}$$

$$\begin{aligned}\frac{\mathrm{d}}{\mathrm{d}t}T(t) = {} & \frac{(T_\mathrm{F}-T)u_1}{1000V} + k_8\eta_1 x_A x_B + k_9\eta_2 x_B x_C \\ & + k_{10}\eta_3 x_C x_P - l_1(T-1000u_2),\end{aligned} \tag{53}$$

$$\frac{\mathrm{d}}{\mathrm{d}t}V(t) = \frac{u_1}{1000}, \tag{54}$$

where the states $x_i(t)$ for $i = A,\ B,\ C,\ P,\ E,\ G$ are the reactant and product concentrations, $T(t)$ represents the reactor temperature and $V(t)$ indicates the reaction liquid volume. The reactions can be controlled by adjusting the feed rate of reactant B, $u_1(t)$, and the cooling jacket temperature, $u_2(t)$.

Constraints. An upper bound of 90°C is imposed to prevent thermal runaway, while a lower bound of 60°C is put in place to avoid phase transitions inside the reactor:

$$60^\circ\mathrm{C} \leqslant T(t) \leqslant 90^\circ\mathrm{C}. \tag{55}$$

Uncertainty on two key parameters, i.e., the feed temperature T_F and the heat transfer coefficient l_1 between the reactor and the cooling jacket, is taken in consideration. These two parameters directly affect the reactor temperature T as can be seen from Eq. (53). It is assumed that the uncertainty on the two considered parameters is described by a Gaussian distribution with a standard

Journal homepage: http://www.journals.elsevier.com/expert-systems-with-applications
Original file available at: http://www.sciencedirect.com/science/article/pii/S0957417415003747

Postprint version of paper published in Expert Systems with Applications 2015, vol. 42, p. 7710-7731.
The content is identical to the published paper, but without the final typesetting by the publisher.

deviation of 10% of the actual mean value. The Sigma Point method allows calculating the reactor temperature's *expected value* $\bar{T}$ and the relative *variance-covariance* matrix $\mathbf{P}_{\mathrm{T}}$ by propagating the uncertainty on the two parameters through the nonlinear dynamic system, i.e., Eqs. (47)-(54). It is now possible to achieve a higher level of robustness, i.e., a lower operation risk, by imposing the constraint expressed in Eq. (55) in analogy with the constraint formulation reported in Eq. (45) as:

$$\bar{T} - \alpha_{\mathrm{T}} \sqrt{\mathbf{P}_{\mathrm{T}}} \geqslant 60^{\circ}\mathrm{C}, \tag{56}$$

$$\bar{T} + \alpha_{\mathrm{T}} \sqrt{\mathbf{P}_{\mathrm{T}}} \leqslant 90^{\circ}\mathrm{C}. \tag{57}$$

It has to be noted that in this case the *variance-covariance* matrix $\mathbf{P}_{\mathrm{T}}$ collapses to a scalar value since it is only calculated for the reactor temperature differential state T. In analogy with Eq. (45), this formulation can be interpreted as a single *chance constraint* and it allows considering the maximization of α_{T} directly as an objective function leading to (i) the minimization of operational risk and (ii) the *trade-offs* evaluation with the other investigated objective functions. The normality assumption can be afterwards checked via dedicated Monte Carlo realizations before implementing a selected solution in real-life.

Objective functions. Originally, a global objective function simultaneously considering the maximization of the product P and E was proposed (**?**). Successively, a multi-objective formulation considering the maximization of P and E as individual objectives was proposed in **?**. In the current work, five different objective functions are simultaneously considered. In particular, the five individual objective functions are: (i) the maximization of product P, (ii) the maximization of product E, (iii) the minimization of waste product G, (iv) the minimization of the total batch time t_{f}, and (v) the minimization of operational risks, i.e., the maximization of α_{T}. These five objective functions can be

Journal homepage: http://www.journals.elsevier.com/expert-systems-with-applications
Original file available at: http://www.sciencedirect.com/science/article/pii/S0957417415003747

Postprint version of paper published in Expert Systems with Applications 2015, vol. 42, p. 7710-7731.
The content is identical to the published paper, but without the final typesetting by the publisher.

mathematically expressed as follows:

$$J_1 = -x_E(t_\mathrm{f})V(t_\mathrm{f}), \tag{58}$$

$$J_2 = -x_P(t_\mathrm{f})V(t_\mathrm{f}), \tag{59}$$

$$J_3 = x_G(t_\mathrm{f})V(t_\mathrm{f}), \tag{60}$$

$$J_4 = t_\mathrm{f}, \tag{61}$$

$$J_5 = -\alpha_\mathrm{T}. \tag{62}$$

It has to be noted that the optimization problem is formulated in a minimization framework, hence, a minus sign is assigned to objective functions J_1, J_2 and J_5 in order to ensure their maximization. The five objectives considered cover the three pillars of *sustainable development*. It can be seen that the maximization of product E (i.e., J_1) and P (i.e., J_2) and the minimization of batch time (i.e., J_4), are directly related to the economic sustainability aspect, while the minimization of waste product G (i.e., J_3), and of operational risks (i.e., maximization of J_5) are related to environmental and societal sustainability aspects. The minimization of operational risk (i.e., reducing the chances of hazardous situations) allows to directly quantify the arising *trade-offs* between the increase in robustness of the process operation and the more economically and environmentally oriented objective functions.

In order to maintain the number of considered objectives in a suitable range to allow the user to gain the most information out of it without overloading him/her (**??**), reduction techniques like Principle Components Analysis (PCA) (**?**), Self Organizing Maps (SOM) **?** or others can be considered. Additionally, as a general remark it is appropriate to formulate objective functions that have a clear (bio)chemical interpretation or specific measures that are used in the field of the investigated problems.

The presented RMOOCP problem constitutes of 50 ODEs. The problem is

Journal homepage: http://www.journals.elsevier.com/expert-systems-with-applications
Original file available at: http://www.sciencedirect.com/science/article/pii/S0957417415003747

Postprint version of paper published in Expert Systems with Applications 2015, vol. 42, p. 7710-7731.
The content is identical to the published paper, but without the final typesetting by the publisher.

subsequently reformulated into an NLP according to the OCoL method with a 4th order Lagrange polynomial and 50 piecewise constant intervals. The resulting NLP presents 8101 decision variables of which 101 are degrees of freedom for the optimizer. Hence, a total of 8000 equality and 300 inequality constraints are imposed. The solution of one NLP corresponds to a Pareto point on the front and it is typically achieved in less than 10 s, which, hence, enables real-time decision-making.

3.3. The Pareto Browser graphical user interface

The case study introduced in the previous section is used to actively introduce the *Pareto Browser*. At first only J_1, J_3 and J_5 are considered in order to be able to start with a 3D visualization (which is a more familiar visualization for most of the DMs). The results for the complete five-objective problem along with the dedicated features of the *Pareto Browser* for high-dimensional problems are reported in Section 4.

Figure 3 depicts the standard screenshot that appears when a RMOOCP is solved with the *Pareto Browser*. The decision-maker can click points that are of particular interest to him/her on the left plot. These points will then be highlighted in the Pareto front while the corresponding state and control profiles will be plotted, with matching colors, on the right part of the main figure (see Figure 3). Additionally, the confidence region (CR) associated with the value of the *back-off* parameter α_T is plotted for each of the state profiles as it can be seen in the right part of the Figure 3. In particular, it is possible to notice the difference in the reactor temperature profile T induced by the different robustness levels adopted for the two points. In fact, the confidence region related to the solution highlighted in dark grey is much larger than the one corresponding to the Pareto point identified with a light grey color. Hence, a lower operational risk is achieved when the batch reactor is run according to the Pareto point highlighted in dark grey. The *radio buttons* on the right allow visualizing different states and controls. The number of *radio buttons* next to

Journal homepage: http://www.journals.elsevier.com/expert-systems-with-applications
Original file available at: http://www.sciencedirect.com/science/article/pii/S0957417415003747

Postprint version of paper published in Expert Systems with Applications 2015, vol. 42, p. 7710-7731.
The content is identical to the published paper, but without the final typesetting by the publisher.

the state and control plots is respectively given by the number of states and controls of the investigated case study, i.e., for this case eight states and two controls.

The different functionalities of the *Pareto Browser*, i.e., one for each of the depicted buttons in Figure 3, are illustrated by actively solving the considered problem. In this way the reader can better understand the general idea under which the *Pareto Browser* decision-support tool was designed. The first feature that a DM can use is the *Add all centroids*. By clicking on this button all the centroids of the triangles reported in Figure 3 are calculated. This results in a finer discretization of the Pareto front allowing the DM to evaluate different regions of the *Pareto set* before expressing his/her preferences. In this case four additional points are added to the Pareto front, each of the points is the solution of a dedicated NLP of the size reported in Section 3.2. The *Add centroid* button adds only one centroid that can be interactively selected via a pop-up window. An example of this is reported in the next section (Section 4) for a five-objective case study.

After exploring the various alternatives, the DM settles his/her interest for the region in between the two highlighted points in Figure 4. In particular, the DM is satisfied with the level of robustness of both the points highlighted in light grey and the one highlighted in dark grey. However, the DM is willing to compromise on the amount of production of component E in order to reduce the production of the unwanted by-product G. To achieve a solution that expresses his/her preferences best, the DM can proceed in different ways.

For instance, if the DM wishes to obtain an exploration point in the region of interest between the two highlighted points he/she can click on the *Estimate point* button. Then, the top plot in Figure 5 pops up on the screen and the DM can move the star marker to the desired location for the estimated point. The position of the star marker is determined with the use of the two sliders on the bottom of the left plot in Figure 5. It is worth to point out that, only two

Journal homepage: http://www.journals.elsevier.com/expert-systems-with-applications
Original file available at: http://www.sciencedirect.com/science/article/pii/S0957417415003747

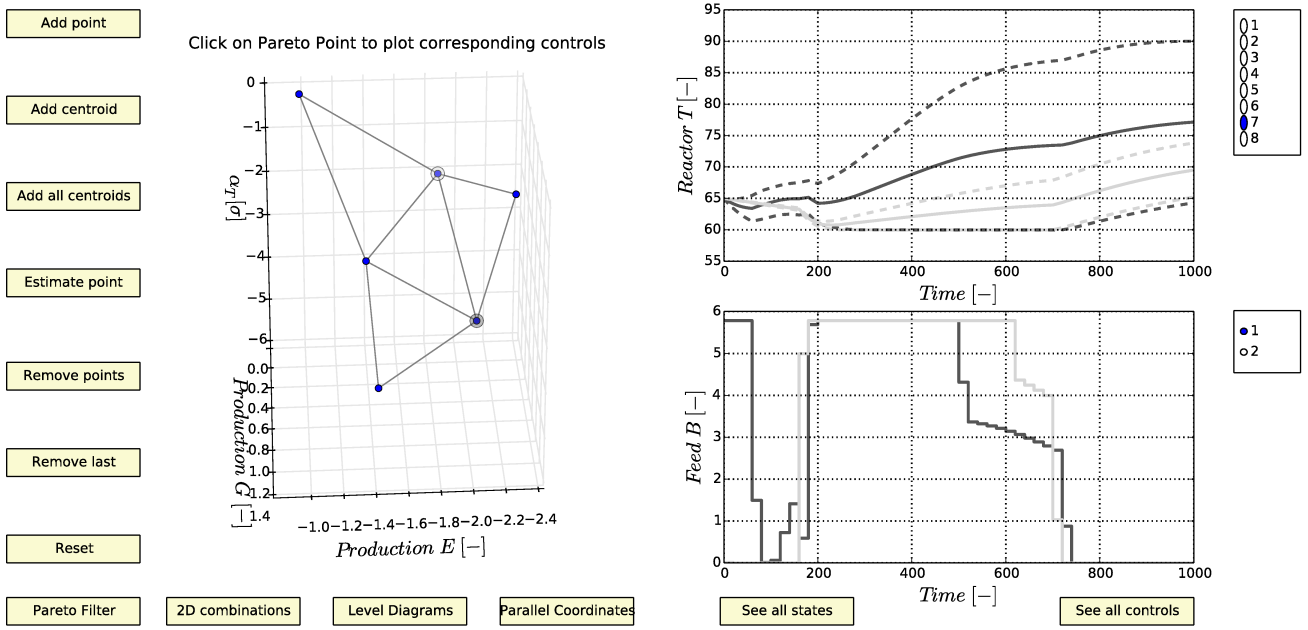

Figure 3: *Pareto Browser*'s main figure for a three-objective case. On the left, a graphical representation of the Pareto front is given. On the right, two graphs for plotting states and controls can be observed. Two points on the Pareto front (left plot) are highlighted. The two graphs on the right plot display each time one state (top right graph) or control (bottom right graph).

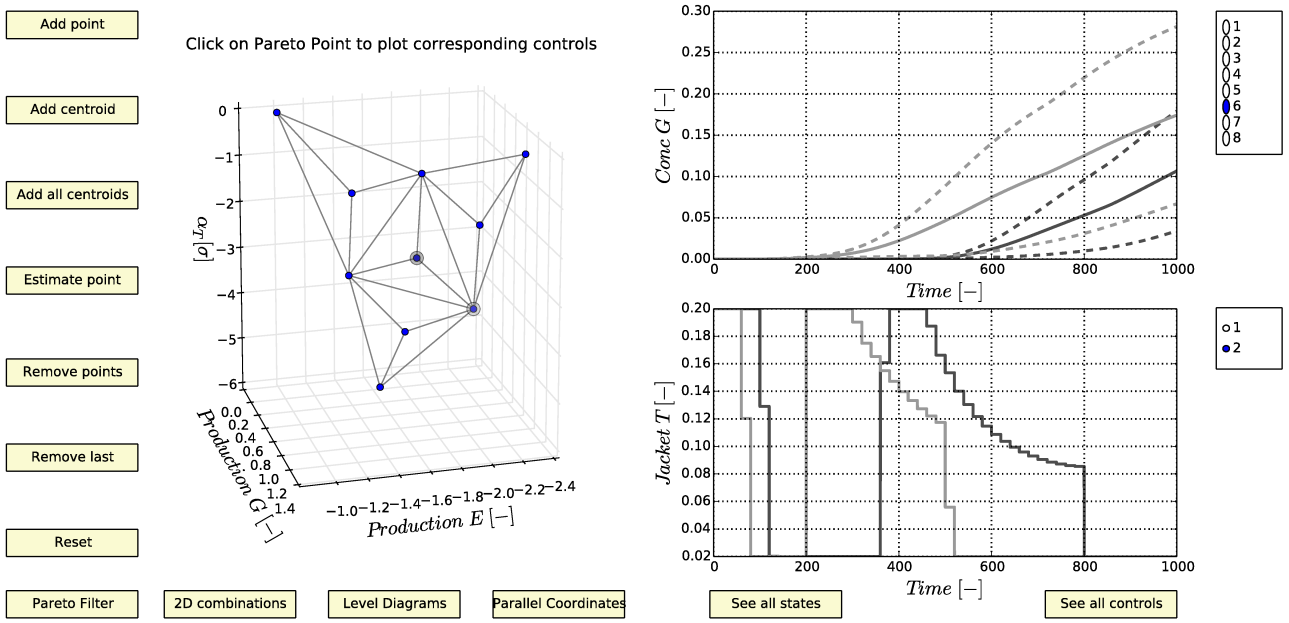

Figure 4: The centroid of every triangle shown in the previous figure is calculated and plotted. This results in a more evenly discretization of the Pareto front.

Postprint version of paper published in Expert Systems with Applications 2015, vol. 42, p. 7710-7731.
The content is identical to the published paper, but without the final typesetting by the publisher.

out of three weights can be directly manipulated, the third one is calculated as a complement to 1 in respect to the one specified by the sliders. This is implemented to ensure that the assumption of convex weights holds. Once the *Confirm* button is clicked, the estimated point is added to the main graph and is identified by a diamond marker (see bottom graph in Figure 5). However, it has to be noted that an estimated point is not obtained via a solution of an optimization problem and, hence, it will not be a Pareto optimal point.

To check whether the estimated point represents his/her expectations, the DM can use one of the alternative visualizations available in the *Pareto Browser*. Figure 6 is triggered when the *Level diagram* button is clicked. In particular, all the Pareto points present in the bottom plot in Figure 5 are also reported here. The *Level diagram* button generates a plot with m different graphs, one for each of the considered m objective functions. Each graph depicts on the y-axis the distance between each Pareto point and the utopia point while on the x-axis a different objective function is reported for each graph. The main advantage of this visualization strategy is that points remain at the same y-axis level in each of the different plots. Moreover, Figure 6 is also interactive and allows highlighting the reported points. With this plot the DM can more easily assess if the estimated point represents his/her preferences.

For example, in this case the estimated point is located between the two highlighted points in all the three subplots of Figure 6. Moreover, the estimated point retains a significant value for the production of the component E and it is still inside the desired values for the *back-off* parameter α_{T}. Finally, the considered estimated point also achieves a considerable reduction of the production of the unwanted component G. Hence, it can be stated that the estimated point corresponds to the DM's preferences. Then, the DM can decide to convert the estimated point into an optimization solution, i.e., to compute a corresponding Pareto point. This can be done by clicking on the *Add point* button. This action gives rise to a plot similar to the one used to generate the estimated point (top plot in Figure 5). By moving the star marker in Figure 7 in the

Journal homepage: http://www.journals.elsevier.com/expert-systems-with-applications
Original file available at: http://www.sciencedirect.com/science/article/pii/S0957417415003747

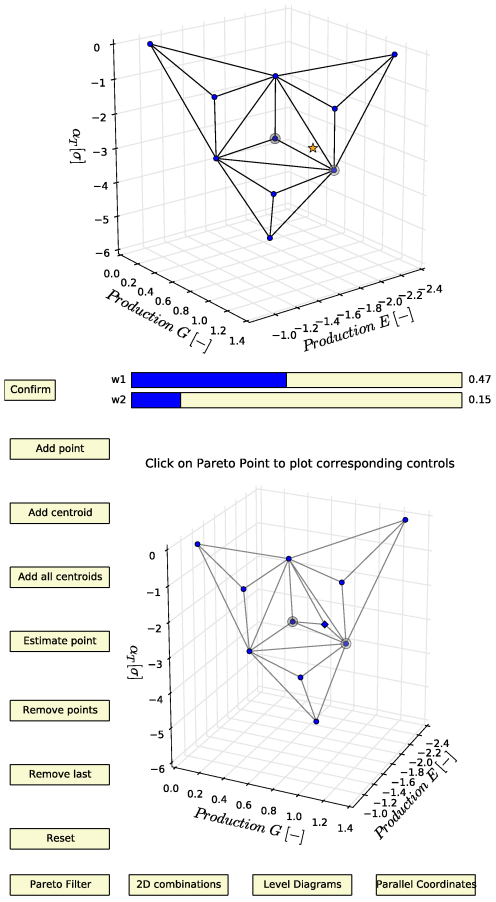

Figure 5: On top the pop up graph obtained by clicking on the *Estimate point* button. By manipulating the two sliders the star marker moves on the graph. Once the *Confirm* button is clicked the estimated point is calculated and added on the main *Pareto Browser*'s figure according to the selected weights. The estimated point, depicted as a diamond, is reported in the bottom plot.

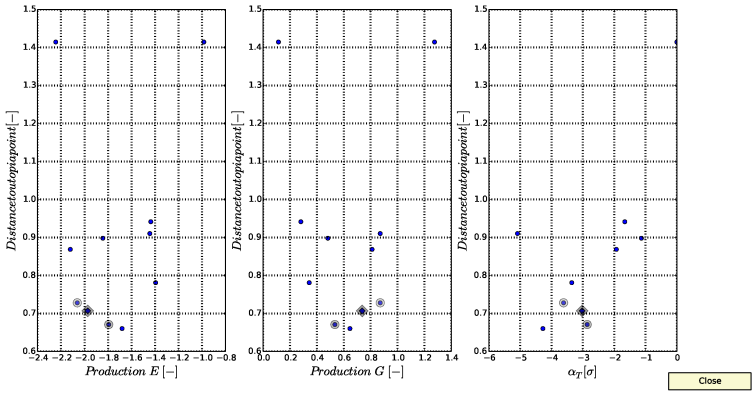

Figure 6: Level diagrams: Every graph displays one objective function on the x-axis and the distance from the utopia point for every solution in the Pareto front on the y-axis. In this visualization strategy each point retains the same y coordinates in every graph.

neighborhood of the estimated point (diamond) an clicking the *Confirm* button an NLP is formulated according to the specified scalarization parameter vector $\mathbf{w}_{\text{add}} = [0.46\ 0.16\ 0.27]^\intercal$ and solved. The result of the NLP is a Pareto point, highlighted in black, and it substitutes the estimated point on the main *Pareto Browser* (Figure 8).

To verify that the last added point corresponds to his/her preferences the DM can make use of another visualization method by clicking on the *2D combination* button. This button depicts all the possible (non-ordered) 2D combinations between the considered objectives. Hence, for this case Figure 9 reports three subplots, one for each of the (non-ordered) 2D objective function combinations. As can be seen, the last added point highlighted in black is located between the other two highlighted points in all three subplots. Additionally, by clicking on the *Plot all states* and *Plot all controls* buttons, the DM can check that the lastly added solution reflects indeed the desired trends and profiles for all states (see Figure 10) and controls (see Figure 11).

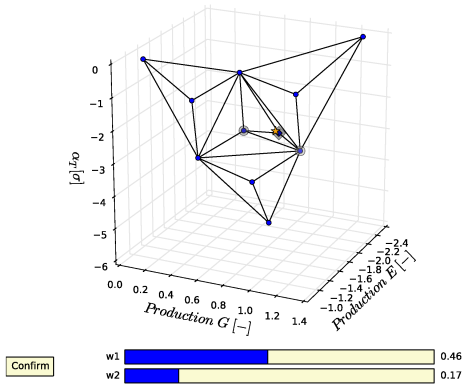

Figure 7: The plot depicts the interactive window that allows selecting the point to be added. By moving the two *sliders* at the bottom the position of the new point, defined by the star marker, will change. When the marker has reached a desired position, one can click the *Confirm* button to calculate the corresponding Pareto point via the formulation and solution of a dedicated optimal control problem according to the scalarization parameter vector $\mathbf{w}_{\text{add}} = [0.46\ 0.16\ 0.27]^\intercal$.

From both Figure 10 and 11 it is possible to appreciate that the black profiles, corresponding to the last added Pareto point (also highlighted in black in Figure 8 and 9), systematically fall between the light grey and dark grey profiles corresponding to the other two solutions similarly highlighted. Therefore, it is possible for the DM to draw a final conclusion whether the point corresponds to his/her preferences or if further additional points are needed. From Figure 10 and 11 it is also possible to identify the *trade-offs* between the objective functions. In particular, the more the feed of the reactant B is delayed in time, the more product E is formed at the expense of the unwanted product G. Moreover, an increasing value of the *back-off* parameter α_{T} and, hence, and increasing level of robustness causes more production of the unwanted product G and less production of the desired product E. However, a safer operation is achieved as can be seen from (i) the reactor temperature profiles T in Figure 10 and from (ii) the shifting towards the beginning of the batch of the constrained control arc for the jacket temperature in Figure 11. Finally, the longer the jacket temperature is kept high at the beginning of the batch, the more of product E

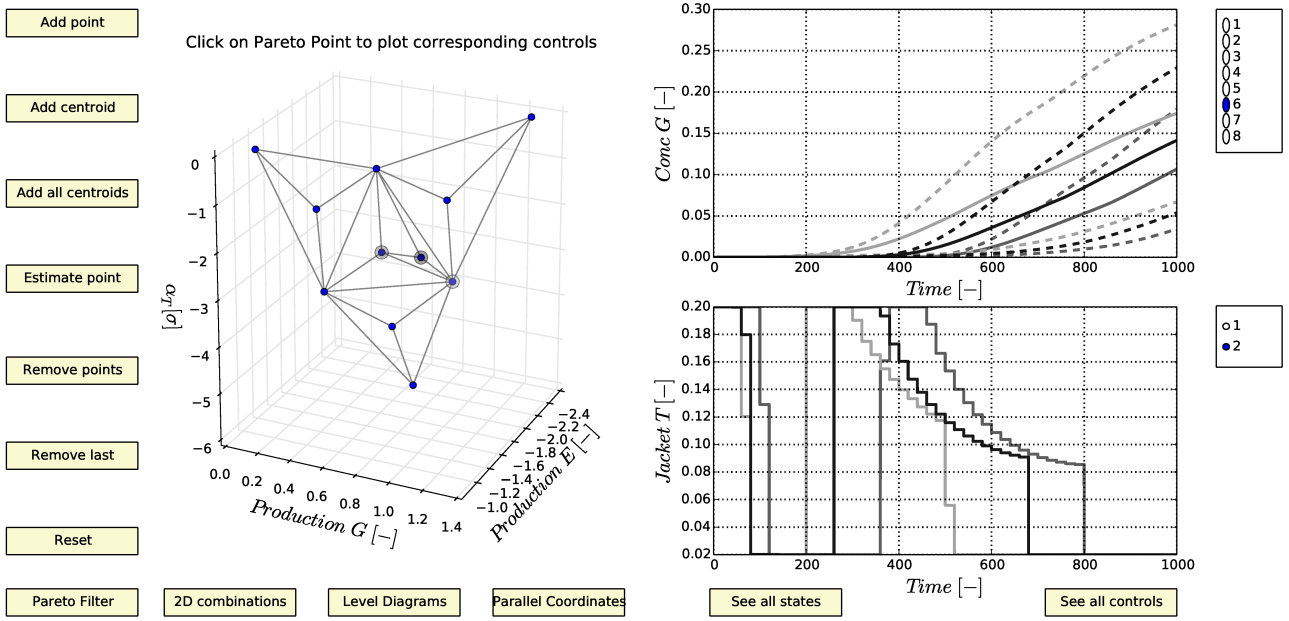

Figure 8: The estimated point in the right plot in Figure 5 is substituted with a Pareto point optioned from the solution of an NLP formulated according to the DM's preferences expressed by moving the star marker in the dedicated pop-up Figure 7.

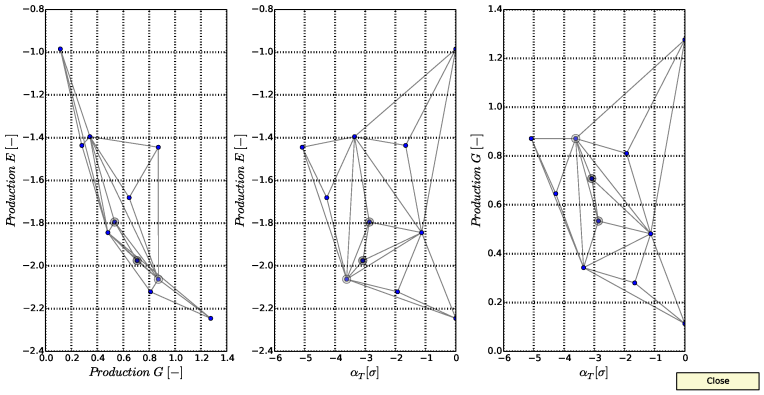

Figure 9: All three (non-ordered) 2D objective function combinations are reported. Hence, in every graph, two out of three objective functions are displayed and can be compared.

is formed.

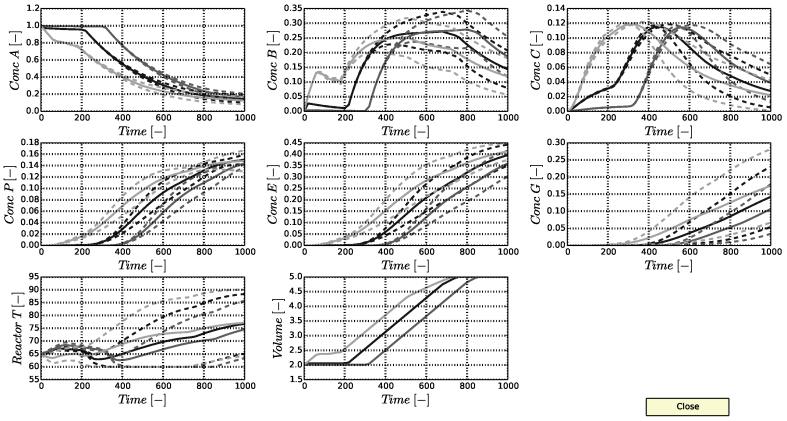

Figure 10: The graph is constituted of eight subplots, i.e., one for each differential state. In particular, in each subplot three different profiles along with the corresponding confidence regions (CRs) are depicted, i.e., one for each of the highlighted points in Figure 8 and Figure 9.

Postprint version of paper published in Expert Systems with Applications 2015, vol. 42, p. 7710-7731.
The content is identical to the published paper, but without the final typesetting by the publisher.

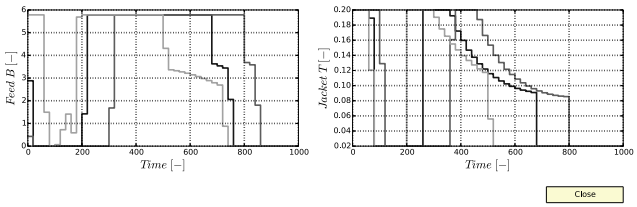

Figure 11: The graph is constituted of two subplots, i.e., one for each control variable described in the problem in Section 3.2. In particular, in each subplot three different trends are depicted, i.e., one for each of the highlighted points in Figure 8.

4. Extension to high-dimensional problems: A five-objective case study with uncertain parameters

In this section the case study presented in Section 3.2 is solved while simultaneously considering all five objectives (Eqs. (58)-(62)). This allows presenting the interactive features of the *Pareto Browser* for high-dimensional problems. In the *Pareto Browser*, *parallel coordinates* (**?**) (PC) is the predefined method of visualization when a problem with more than three objectives is solved. In this visualization method each line represents an n-dimensional point, where n is the number of the parallel axes present in the plot. The parallel coordinates visualization allows the DM to see the *trade-offs* between several objectives at once. Moreover, parallel coordinates, when applied to multi-objective optimization, allows detecting non-Pareto optimal points. As there should always be a *trade-off* between objectives, it is a necessary condition for Pareto optimal points to have crossing lines in their parallel coordinates representation.

As in Section 3.3 the different functionalities are introduced via the search for one preferred solution. In particular, Figure 12 depicts the starting *Pareto set* constituted of 15 Pareto solutions, of which five are the *anchor points* and the remaining 10 represent intermediate solutions between couples of *anchor points*. As can be seen from Figure 12 the right part of the *Pareto Browser*, where states and controls are plotted, is exactly the same as the one for the 3D case. The possibility of highlighting points and plotting corresponding state and

Journal homepage: http://www.journals.elsevier.com/expert-systems-with-applications
Original file available at: http://www.sciencedirect.com/science/article/pii/S0957417415003747

Postprint version of paper published in Expert Systems with Applications 2015, vol. 42, p. 7710-7731.
The content is identical to the published paper, but without the final typesetting by the publisher.

control profiles is retained as most of the other functionalities. However, the *Add all centroids* button is not present anymore. This is due to the lack of the possibility to efficiently visualize five dimensional simplices in the Parallel Coordinates plot. Additionally, given the large number of solutions the use of colors to highlight the different points and solutions is necessary in high-dimensional problems.

For this case study it is assumed that the DM is primarily interested in investigating the effect of the two objective functions added here, i.e., J_2 maximizing the production of P and J_4 minimizing the *batch time* t_{f}, respectively defined in Eqs. (59) and (61). At first the DM expresses the preference to investigate the *trade-off* between reducing operational risk and maximizing J_2. In this respect, the highlighted point in Figure 12 depicts the *anchor point* for objective J_2 (blue line) and the intermediate point between this solution and the *anchor point* for the maximization of α_{T}. In other words the two highlighted points were respectively obtained with the following scalarization parameter vectors $\mathbf{w}_{\mathrm{blue}} = [0.0\ 1.0\ 0.0\ 0.0\ 0.0]^{\intercal}$ and $\mathbf{w}_{\mathrm{yellow}} = [0.0\ 0.5\ 0.0\ 0.0\ 0.5]^{\intercal}$.

As it can be seen from the corresponding reactor temperature profiles reported in the top right graph in Figure 12, the robustification effect is quite significant. In fact, the yellow temperature profile lies quite distant from the bottom constraint, while the blue temperature profile touches the bottom constraint. It is also possible to notice the constrained arc defined in the blue control profile (right bottom plot in Figure 12) corresponding to the period of time when the bottom temperature constraint is active. Then, if for instance neither of the highlighted solutions satisfy the DM (i.e., the yellow one does not produce enough P and the blue one does not reduce the operational risk enough) a compromise solution can be generated by clicking on the *Add centroid* button).

The *Add centroid* button launches a new figure (i.e., Figure 13) in which the DM can click on a certain number of points. He/she should click on the points

Journal homepage: http://www.journals.elsevier.com/expert-systems-with-applications
Original file available at: http://www.sciencedirect.com/science/article/pii/S0957417415003747

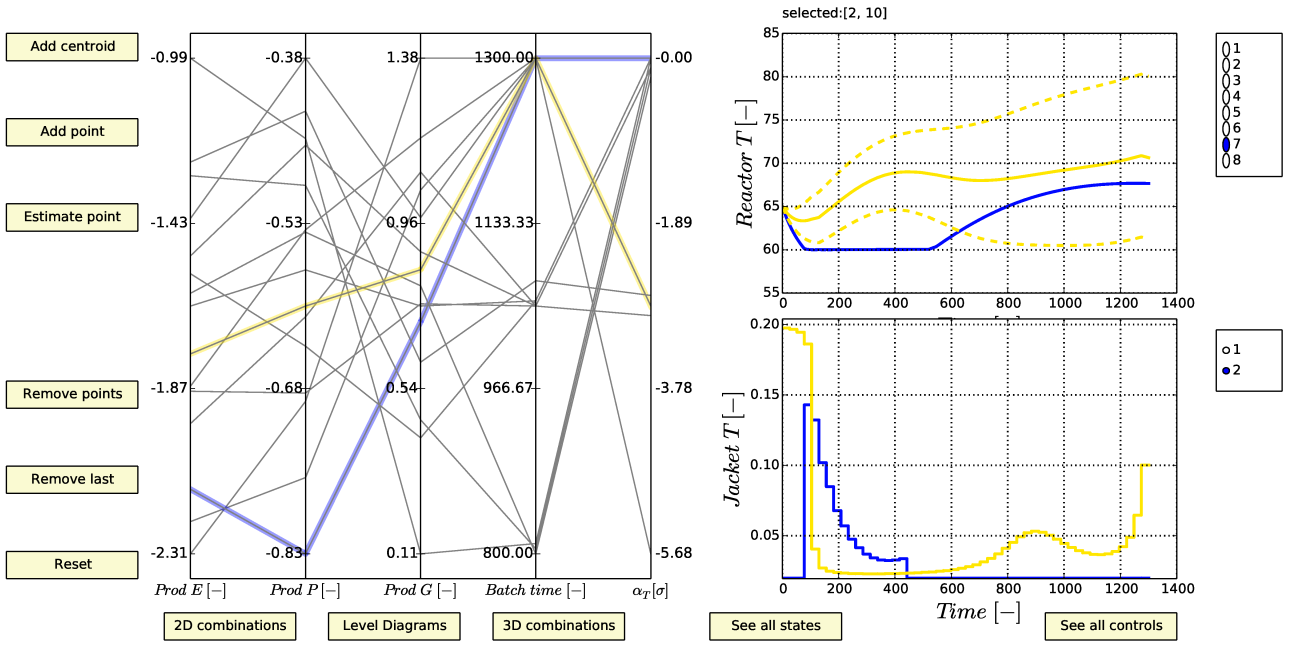

Figure 12: Similarly to the 3D visualization, one can highlight points. However, in the parallel coordinates representation, optimal solutions (points) are represented by lines, so these lines are highlighted.

Postprint version of paper published in Expert Systems with Applications 2015, vol. 42, p. 7710-7731.
The content is identical to the published paper, but without the final typesetting by the publisher.

that are most interesting according to his/her preferences such that the centroid of the n-dimensional object identified by the clicked points can be calculated. The number of points that can be clicked is limited to the number of objective functions, i.e., the dimension of the problem. The centroid is calculated as follows:

$$P_{est} = \frac{\sum_{i=1}^{n} P_i}{n} \qquad n = \#\text{ clicked points} \tag{63}$$

In this case the DM selects the two previously highlighted points in Figure 12. The markers of the point selected change from blue circles to orange triangles and the approximation of the solution that will be calculated is identified by a black star marker. As can be seen in Figure 13, the points remain highlighted in the new plotted window. This allows an easier selection process for the DM. Moreover, the DM can choose with the radio button on the top left three different visualization methods under which he/she can select points, i.e., 2D, 3D and parallel coordinates. In Figure 13 the 2D representation is used. Similarly to the *2D combination* graph in Figure 9 also here the 2D (non-ordered) combinations of objective functions are plotted. In complete analogy, the 3D radio button will generate a graph with a plot for each of the possible 3D (non-ordered) combinations of objective functions. However, it has to be noted that for 5 (or more) objectives this latter option is not so interesting since the same number of 2D and 3D (non-ordered) combinations of objective functions is generated. (For more than five objectives the number 3D combinations even exceeds the number of 2D combinations.) Hence, the 2D button allows representing the same amount of information with equal or less plots. Alternatively, a parallel coordinates representation similar to the left plot of Figure 12 can be used to select the preferred solutions.

The solution obtained as a result of the *Add centroid* button is highlighted in red in Figure 14 and it is characterized by the scalarization parameter vector $\mathbf{w}_{\text{centroid 1}} = [0.0\ 0.75\ 0.0\ 0.0\ 0.25]^{\intercal}$. The achieved solution is, as expected,

Journal homepage: http://www.journals.elsevier.com/expert-systems-with-applications
Original file available at: http://www.sciencedirect.com/science/article/pii/S0957417415003747

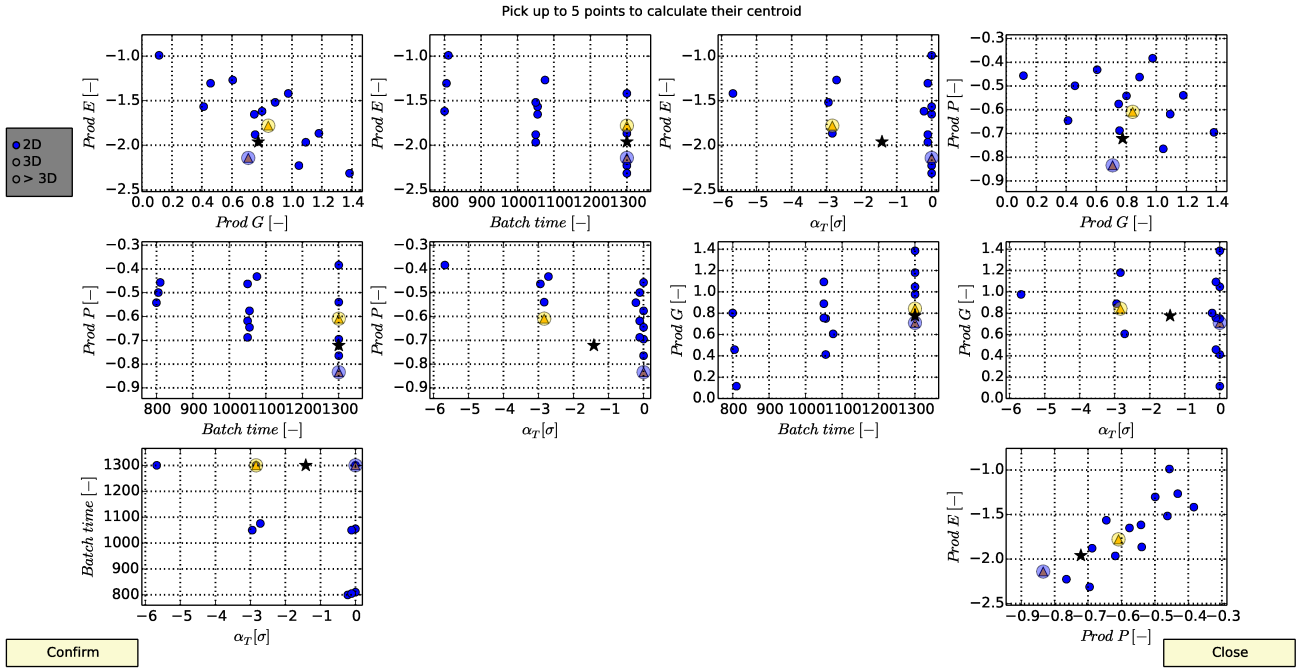

Figure 13: Figure to decide where a new solution should end up. One can click the already calculated points, identified with blue circles, to select them. The solutions selected to be part of the n-dimensional object turn into orange triangles. The centroid of the n-dimensional object generated by the selected point is calculated and depicted with a black star marker.

situated in between the two starting points. Also the corresponding reactor temperature T profile and feed of reactant B in the top and bottom right plots in Figure 14 reflect the compromising nature of the added Pareto solution. Interesting to notice is, as observed in Section 3.3 for the production of E, that the earlier the reactant B is fed into the reactor, the more product P is formed.

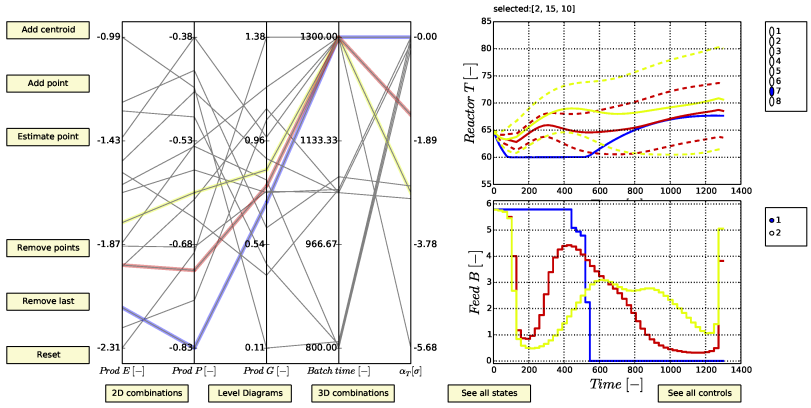

Figure 14: The figure reports the added points calculated based on the preferences expressed by the DM in Figure 13. The added point is highlighted in red and the corresponding reactor temperature T and the reactant B feed rate profile are reported in the dedicated plots (also in red). As expected the obtained solution is located in the middle between the two starting points.

The DM can now decide to obtain a selection of points in the identified interesting region according to his/her preferences, i.e., in this case between solutions highlighted in blue and yellow. After several points have been added to the graph it might become difficult to clearly decide among the added solutions. Hence, the ones that do not completely satisfy the DM's preferences can be easily removed by clicking on the *Remove points* button. This action causes a secondary plot reported in Figure 15 to be generated. In this graph all the generated solutions are starting solutions and are reported in light grey. The highlighted solutions remain highlighted. It has to be noted that here the solution previously highlighted in yellow is now highlighted in a light green color.

This is because the highlighting colors are dynamically assigned to the solutions according to their relative position in the *Pareto set*. Hence, the addition of five solutions to the Pareto front caused the color change. The added solutions are identified by solid blue lines instead, by clicking on the blue lines they turn into dashed orange indicating that they have been selected for removal. In particular, in this case the two solutions to be removed have been selected by the DM since they are both characterized by a too high production of the unwanted component G. By clicking the *Confirm* button the selected solutions are removed.

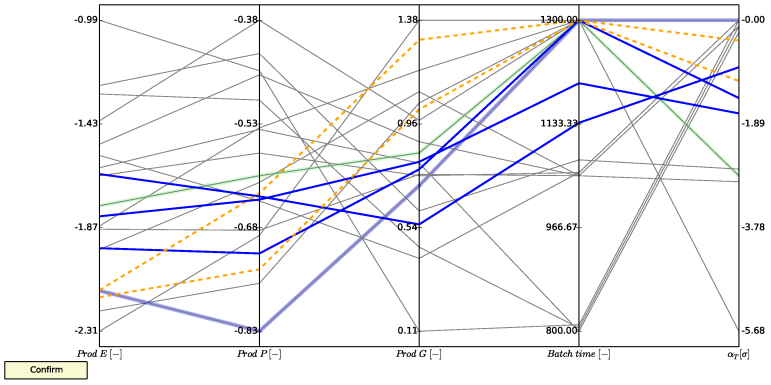

Figure 15: The grey lines represent the 15 starting Pareto points, while the added points are depicted in blue. Only the added point can be removed from the graph. The points estimated to be removed can be selected by clicking on them. When clicked a point turns from a solid blue line into a dashed orange one. When the selection is complete, the removal is completed by clicking on the *Confirm* button.

To complete his/her search the DM decided to add an additional point to the Pareto front. In particular, the point to be added should lie somewhere in the neighborhood of the previously obtained points. The DM could resort to use once again the *Add centroid* button, however, to have some more degrees of freedom he/she decides to use the *Add point* button. This latter button also triggers a decision-support graph (see Figure 16). This plot is the high-dimensional counterpart of the one triggered by the same button in the 3D case

(see Figure 7). Therefore, the working principle is quite similar, i.e., the DM expresses his/her preferences by adjusting the five sliding bars which each correspond to a scalarization parameter related to one of the five objectives. The DM can switch between sliders via the radio button at the top right of the plot. The DM in this case settles for a solution defined by the scalarization parameter vector $\mathbf{w}_{5\text{obj}} = [0.060.400.190.100.25]^\intercal$.

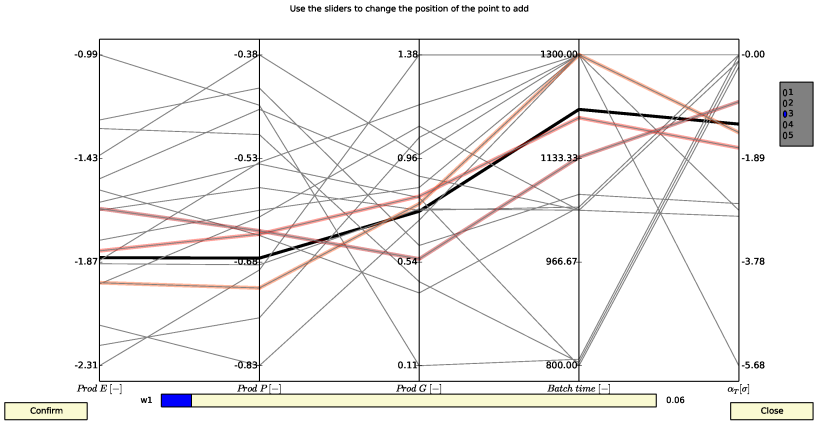

Figure 16: The decision-support triggered by the *Add point* button allows the DM expressing his/her preference by adjusting n sliders, one for each of the n scalarization parameters related to the n considered objective functions. The estimated position of the point is depicted with a black line.

The added point represents the DM's final preference and it compromises between operational risk, production of P, production of the unwanted product G and the final batch time. In fact, the relatively low productivity of both P and E can be compensated by the possibility to run an additional batch in a production campaign due to the shorter batch time. Additionally, the lower operational risk can also contribute to the overall production campaign yield by reducing the amount of faulty batches. Finally, also the *trade-off* introduced by a variable batch time can be quantified. In particular, a shorter batch time leads to a lower production of unwanted product G and a higher production

of P. This is due to the fact that G is the product of the last reaction in the reaction scheme that uses P as a reactant (see Section 3.2).

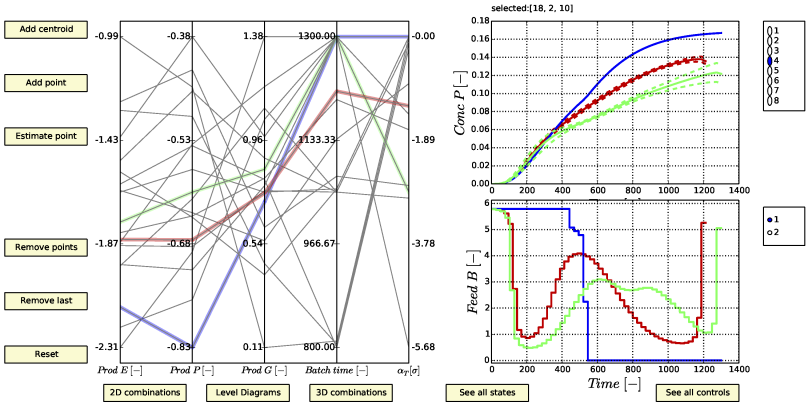

Figure 17: The point corresponding to the one selected by the DM in Figure 16 is calculated via the solution of a dedicated optimal control problem and added to the plot. As can be seen, the added solution (red) is a compromise solution between the two solutions considered at the beginning in Figure 12

.

5. Discussion

This work proposes the *Pareto Browser* as a novel *expert system* tool to support and enable decision-making based on interactive MOO and a GUI to generate insights via interactive visualization methods. During the course of the research needed to implement and test the proposed framework it became clear that additional significant improvements from theoretical, application and software implementation points of view are necessary before a systematic adoption of such tools could be achieved at industrial level. The difficulties of this task arise from the wide interdisciplinary nature of this field of research. In fact, when considering several objectives simultaneously the problem of correctly visualizing and understanding the obtained solutions is directly related to the

Postprint version of paper published in Expert Systems with Applications 2015, vol. 42, p. 7710-7731.
The content is identical to the published paper, but without the final typesetting by the publisher.

field of information and visualization analytics, while the efficient solution of the subtended problem relates to the field of mathematical optimization. Additionally, the design of the human interaction step should be carefully considered also from a psychological point of view, since the used tool should not influence the final decision of the user (**??**). In this section, a discussion of the advantages and drawbacks of the proposed framework is reported and, then, taking this as starting point future research directions are highlighted.

5.1. Advantages and Drawbacks

The different advantages and drawbacks related to the *Pareto Browsers* are going to be discussed in separate paragraphs according to the specific point of view, i.e., optimization, interactivity and visualization. In each paragraph the advantages are going to be listed first followed by the related drawbacks and possible mitigating measures. Finally, a discussion on future research directions is reported. It is important to notice that the final application of the presented tool is the solution of nonlinear dynamic multi-objective optimization problems under uncertainty in real-time, hence, several characteristics of the proposed tool were specifically selected to achieve this goal.

The underlying multi-objective and dynamic optimization algorithm.. The proposed tools make use of an adapted interactive version of well-known scalarization methods (i.e., NBI and ENNC) linked with advanced automatic differentiation methods and fast gradient-based deterministic approaches to solve the considered numerical optimization problems. The advantages of this set-up are: (i) the efficient solution of series of large-scale NLPs arising from the scalarization methods, (ii) the easy definition of complex constraints, (iii) the possibility to deal with many (i.e., more than three) objective functions and (iv) the generation of a well-defined Pareto front. Additionally, the advanced computational capabilities of the proposed framework are certainly needed when the problem size increases due to the incorporation of uncertainty. Possible drawbacks of the implemented methodology relate to: (i) the inability to tackle

Journal homepage: http://www.journals.elsevier.com/expert-systems-with-applications
Original file available at: http://www.sciencedirect.com/science/article/pii/S0957417415003747

Postprint version of paper published in Expert Systems with Applications 2015, vol. 42, p. 7710-7731.
The content is identical to the published paper, but without the final typesetting by the publisher.

objective functions of discontinuous nature, i.e., non-differentiable, (ii) the solution of the problems can only guaranteed to be locally optimal, (iii) the selected scalarization methods can return dominated (non-optimal) Pareto points and (iv) the more extreme regions of the Pareto front are not easily explored in 3D or higher-dimensional cases. Possible ways to mitigate these drawbacks can include the implementation in the proposed tool of globalization strategies (e.g., scatter search (**?**) or evolutionary strategies (**?**)). These techniques can be used in an initial phase of the problem solution and when the DM is satisfied with a more local area of search he/she can decide to switch to deterministic approaches. To achieve the entire exploration of the Pareto front the implementation of the achievement scalarization function can prove beneficial. Evolutionary strategies can also address the shortcoming in solving discontinuous objective functions. However, given the more computationally demanding nature of these latter methods parallelization strategies should be deployed to still achieve a real-time decision-making procedure. Finally, additional Pareto filter types (**?**) to remove dominated solutions and facilitate the decision process can be introduced.

The interactive framework.. As described throughout the paper, the DM interaction within the *Pareto Browser* is achieved via dedicated decision-support plots. In particular, the DM is asked to express his/her preferences by *browsing* the weights space via sliders. This action is directly translated into a projection in the criteria space, hence, the DM can readily see where the point to be added will eventually end up. Additionally, a simplicial grid is fitted on the Pareto front. This grid allows to refine the entire Pareto front at once and to easily add points in higher-dimensional problems. The proposed interaction differs from the other reported in literature for this last two abilities. However, such an interaction may not be the favorite way for the DM to express his/her preferences. In fact the proposed interaction mechanism might require some previous knowledge of multi-objective optimization from the DM. This is in general less required when a reference-based interaction mechanism is implemented (see,

Journal homepage: http://www.journals.elsevier.com/expert-systems-with-applications
Original file available at: http://www.sciencedirect.com/science/article/pii/S0957417415003747

Postprint version of paper published in Expert Systems with Applications 2015, vol. 42, p. 7710-7731.
The content is identical to the published paper, but without the final typesetting by the publisher.

e.g., **??**). The idea of the authors would be to additionally implement in a short future a reference-based approach, i.e., the Achievement Scalarizing Function (ASF). Additionally, it would be beneficial if the DM could freely switch between different solution methodologies. To do so, a mathematical equivalence between the solutions obtained with different methods is desirable. In this respect, the works reported in **?** and **?**, which links solutions of WS, NBI and ENNC, could be extended to the ASF function.

The visualization of multi-dimensional Pareto sets.. One of the major challenges to achieve a mature *expert system* for the solution of high-dimensional multi-objective problems is the proper visualization of the obtained results. In this work this issue is addressed by implementing different visualization strategies which the DM can interactively explore. Additionally, the DM can also switch between the methods to possibly gain different insights which are not at reach in other. The sort of interactive and interchangeable visualization strategy adopted in this work presents some advantages when handling a large amount of objectives. However, all the proposed visualization methods present a common drawback, i.e., the resulting graphs tend to clutter and, hence, lose effectiveness in information transfer. A possible solution to this problem can be the use of more interactive platforms allowing the possibility to construct advanced interaction schemes between the software and the DM. For example web based implementation can prove beneficial in this respect (**?**).

5.2. Future research directions.

Further quantify the societal and environmental aspect.. Nowadays, industry and society are faced with the enormous task to improve themselves focusing not only on the economic aspect but also on the complex human and ecological ones. In this context, it becomes crucial to devise new metrics to incorporate environmental and societal cost functions in optimization frameworks. For the environmental aspect a few interesting strategies exist and successful attempts to introduce them in optimization studies have been reported in literature (e.g.,

Journal homepage: http://www.journals.elsevier.com/expert-systems-with-applications
Original file available at: http://www.sciencedirect.com/science/article/pii/S0957417415003747

Postprint version of paper published in Expert Systems with Applications 2015, vol. 42, p. 7710-7731.
The content is identical to the published paper, but without the final typesetting by the publisher.

??). This is certainly not the same, up to the authors' knowledge, for societal related cost functions. Therefore, an effort should be dedicated to define and introduce societal and environmental metrics that can be adopted in optimization studies. This eventually will lead to tailored tools to empower the new generation of DMs to make more informed, sound and globally beneficial decision.

Use of classification and decision-support methods.. One important limitation of the available interactive multi-objective methods is the ability to efficiently solve complex problems with many objectives (i.e., more than three). In this respect, an important aspect to be considered is the *processing* capabilities of the human DM (??). In the same context, the definition of the way the DM is called to express his/her preferences and the amount of information he/she is required to provide each time becomes crucial (?). Hence, the introduction of classification, data reduction techniques and machine learning algorithms to identify conflicting and synergetic objectives and to appropriately steer the decision process has to be considered for future implementation. A first example of such an approach was presented in ?.

Interactive visualization strategies.. As already highlighted in the course of this work one of the main areas to be further investigated in the context of interactive multi-objective optimization is definitely the appropriate definition of tailored visualization strategies to correctly understand the obtained results especially for problems with many objectives (i.e., more than three) (?). In this respect, the use of a programming environment that allows the definition of highly interactive visualizations can produce a significant added value (?). However, care should be taken in the definition and implementation of this strategy such that the final decision is not influenced by the particular visualization strategy adopted. Hence, the proposed visualization methods should be instrumental to the decision process without invading or disrupting it.

Journal homepage: http://www.journals.elsevier.com/expert-systems-with-applications
Original file available at: http://www.sciencedirect.com/science/article/pii/S0957417415003747

Postprint version of paper published in Expert Systems with Applications 2015, vol. 42, p. 7710-7731.
The content is identical to the published paper, but without the final typesetting by the publisher.

Global multi-objective optimization. One of the limitations of the presented framework is the inability to guaranty the solution of the problem to global optimality. Evolutionary schemes have proven to reach globally optimal solutions, however, they suffer from long computational time. An alternative can be represented by the development of deterministic global multi-objective optimization approaches. In this respect various set based methods have been proposed in literature, e.g., the so-called sandwich or interval methods (e.g. **??**) could be coupled with fast local gradient-based methods to achieve computationally efficient solutions while guaranteeing global optimality. Additionally, further research is needed to improve the existing set based methods from both theoretical and computational point of view.

6. Conclusions

This work has introduced the *Pareto Browser*, a novel interactive decision-support system for the multi-objective optimization of nonlinear dynamic processes with uncertainty. The proposed framework enables, for the first time, considering the operational risk as an objective function delivering a direct *trade-off* evaluation between reducing operational risk and, e.g., reactor productivity and/or energy consumption. Moreover, the possibility to seamlessly visualize state and control profiles for every Pareto point along with the related robustness level has been found crucial to achieve a sound and well-informed final decision. The quantification of the operational risk is achieved via an efficient formulation of the arising robust multi-objective optimization problem based on the sigma point approach. Additionally, the proposed framework makes use of automatic differentiation and fast gradient-based algorithms to facilitate real-time updates of the Pareto front according to the DM's preferences, both these features proved beneficial and highly desirable. The different interactive visualization strategies made available in the proposed framework have been an asset in generating additional insights and support the DM in deciding how to refine his/her preferences. In this respect, the use of a multi-dimensional simplicial

Journal homepage: http://www.journals.elsevier.com/expert-systems-with-applications
Original file available at: http://www.sciencedirect.com/science/article/pii/S0957417415003747

Postprint version of paper published in Expert Systems with Applications 2015, vol. 42, p. 7710-7731.
The content is identical to the published paper, but without the final typesetting by the publisher.

grid allows the DM to quickly update the Pareto set both entirely or locally also for problems with many objectives (i.e., more than three). Finally, the *Pareto Browser* is successfully tested on a chemical engineering optimal control problem with two uncertain parameters and five objective functions. In particular, the *trade-offs* between the considered objective functions were correctly quantified while no additional computational time was spent in uninteresting parts of the *Pareto set* according to the DM's preferences.

Acknowledgments

Mattia Vallerio has a Ph.D. grant of the Agency for Innovation through Science and Technology in Flanders (IWT). Jan Van Impe held the chair Safety Engineering sponsored by the Belgian Chemistry and Life Sciences Federation essenscia. The research was supported by KUL, PFV/10/002 (OPTEC), the Flemish Government via FWO-projects: FWO KAN2013 1.5.189.13, FWO-G.0930.13, the Belgian Federal Science Policy Office: IAP VII/19 (DYSCO).

References

Agrawal, N., Rangaiah, G., Ray, A., & Gupta, S. (2006). Multi-objective optimization of the operation of an industrial low-density polyethylene tubular reactor using genetic algorithm and its jumping gene adaptations. *Industrial and Engineering Chemistry Research*, *45*, 3182–3199.

Andersson, J., Åkesson, J., & Diehl, M. (2012). CasADi – A symbolic package for automatic differentiation and optimal control. In *Recent Advances in Algorithmic Differentiation* (pp. 297–307). Springer Berlin Heidelberg volume 87 of *Lecture Notes in Computational Science and Engineering*.

Antipova, E., Pozo, C., Guillén-Gosálbez, G., Boer, D., Cabeza, L., & Jiménez, L. (2015). On the use of filters to facilitate the post-optimal analysis of the pareto solutions in multi-objective optimization. *Computers & Chemical Engineering*, *74*, 48 – 58.

Journal homepage: http://www.journals.elsevier.com/expert-systems-with-applications
Original file available at: http://www.sciencedirect.com/science/article/pii/S0957417415003747

Postprint version of paper published in Expert Systems with Applications 2015, vol. 42, p. 7710-7731.
The content is identical to the published paper, but without the final typesetting by the publisher.

Azapagic, A., & Clift, R. (1999). The application of life cycle assessment to process optimisation. *Computers and Chemical Engineering*, *23*, 1509 – 1526.

Beiranvand, V., Mobasher-Kashani, M., & Bakar, A. A. (2014). Multi-objective PSO algorithm for mining numerical association rules without a priori discretization. *Expert Systems with Applications*, *41*, 4259 – 4273.

Biegler, L. (2007). An overview of simultaneous strategies for dynamic optimization. *Chemical Engineering and Processing: Process Intensification*, *46*, 1043–1053.

Bock, H., & Plitt, K. (1984). A multiple shooting algorithm for direct solution of optimal control problems. In *Proceedings of the 9th IFAC world congress, Budapest* (pp. 243–247). Pergamon Press.

Bortz, M., Burger, J., Asprion, N., Blagov, S., Böttcher, R., Nowak, U., Scheithauer, A., Welke, R., Küfer, K.-H., & Hasse, H. (2014). Multi-criteria optimization in chemical process design and decision support by navigation on pareto sets. *Computers and Chemical Engineering*, (pp. 354 – 363).

Bostock, M., Ogievetsky, V., & Heer, J. (2011). D3 data-driven documents. *IEEE Transactions on Visualization and Computer Graphics*, *17*, 2301–2309.

Chaudhuri, S., & Deb, K. (2010). An interactive evolutionary multi-objective optimization and decision making procedure. *Applied Soft Computing*, *10*, 496 – 511.

Das, I., & Dennis, J. (1997). A closer look at drawbacks of minimizing weighted sums of objectives for Pareto set generation in multicriteria optimization problems. *Structural Optimization*, *14*, 63–69.

Das, I., & Dennis, J. (1998). Normal-Boundary Intersection: A new method for generating the Pareto surface in nonlinear multicriteria optimization problems. *SIAM Journal on Optimization*, *8*, 631–657.

Journal homepage: http://www.journals.elsevier.com/expert-systems-with-applications
Original file available at: http://www.sciencedirect.com/science/article/pii/S0957417415003747

Postprint version of paper published in Expert Systems with Applications 2015, vol. 42, p. 7710-7731.
The content is identical to the published paper, but without the final typesetting by the publisher.

Datskov, I., Ostrovsky, G., Achenie, L., & Volin, Y. (2006). An approach to multicriteria optimization under uncertainty. *Chemical Engineering Science*, *61*, 2379 – 2393.

Deb, K. (2001). *Multi-Objective Optimization Using Evolutionary Algorithms*. Chichester, London, UK: John Wiley.

Deb, K., & Jain, H. (2014). An evolutionary many-objective optimization algorithm using reference-point-based nondominated sorting approach, part i: Solving problems with box constraints. *Evolutionary Computation, IEEE Transactions on*, *18*, 577–601.

Deb, K., Mitra, K., Dewri, R., & Majumdar, S. (2004). Towards a better understanding of the epoxy-polymerization process using multi-objective evolutionary computation. *Chemical Engineering Science*, *59*, 4261 – 4277.

Dellnitz, M., Schütze, O., & Hestermeyer, T. (2005). Covering pareto sets by multilevel subdivision techniques. *Journal of optimization theory and applications*, *124*, 113–136.

Diwekar, U. M., & Kalagnanam, J. R. (1997). Efficient sampling technique for optimization under uncertainty. *AIChE Journal*, *43*, 440–447.

Eichfelder, G. (2009). Scalarizations for adaptively solving multi-objective optimization problems. *Computational Optimization and Applications*, *44*, 249–273.

Eskelinen, P., Miettinen, K., Klamroth, K., & Hakanen, J. (2010). Pareto navigator for interactive nonlinear multiobjective optimization. *OR Spectrum*, *32*, 211–227.

Fowler, J. W., Gel, E. S., Köksalan, M. M., Korhonen, P., Marquis, J. L., & Wallenius, J. (2010). Interactive evolutionary multi-objective optimization for quasi-concave preference functions. *European Journal of Operational Research*, *206*, 417 – 425.

Journal homepage: http://www.journals.elsevier.com/expert-systems-with-applications
Original file available at: http://www.sciencedirect.com/science/article/pii/S0957417415003747

Postprint version of paper published in Expert Systems with Applications 2015, vol. 42, p. 7710-7731.
The content is identical to the published paper, but without the final typesetting by the publisher.

Geletu, A., & Li, P. (2014). Recent developments in computational approaches to optimization under uncertainty and application in process systems engineering. *ChemBioEng Reviews*, *1*, 170 –190.

Gong, D., Ji, X., Sun, J., & Sun, X. (2014). Interactive evolutionary algorithms with decision-makers preferences for solving interval multi-objective optimization problems. *Neurocomputing*, *137*, 241 – 251.

Gong, D., Sun, J., & Ji, X. (2013). Evolutionary algorithms with preference polyhedron for interval multi-objective optimization problems. *Information Sciences*, *233*, 141 – 161.

Hannemann, R., & Marquardt, W. (2010). Continuous and discrete adjoints for the hessian of the lagrangian in shooting algorithms for dynamic optimization. *SIAM Journal on Scientific Computing*, *31*, 4675 – 4695.

Hartikainen, M., Miettinen, K., & Wiecek, M. M. (2012). Paint: Pareto front interpolation for nonlinear multiobjective optimization. *Computational Optimization and Applications*, *52*, 845–867.

Hartwich, A., & Marquardt, W. (2010). Dynamic optimization of the load change of a large-scale chemical plant by adaptive single shooting. *Computers and Chemical Engineering*, *34*, 1873 – 1889.

Hassanzadeh, F., Nemati, H., & Sun, M. (2014). Robust optimization for interactive multiobjective programming with imprecise information applied to r&d project portfolio selection. *European Journal of Operational Research*, *238*, 41 – 53.

Hettenhausen, J., Lewis, A., & Kipouros, T. (2014). A web-based system for visualisation-driven interactive multi-objective optimisation. *Procedia Computer Science*, *29*, 1915–1925. 2014 International Conference on Computational Science.

Journal homepage: http://www.journals.elsevier.com/expert-systems-with-applications
Original file available at: http://www.sciencedirect.com/science/article/pii/S0957417415003747

Postprint version of paper published in Expert Systems with Applications 2015, vol. 42, p. 7710-7731.
The content is identical to the published paper, but without the final typesetting by the publisher.

Houska, B., & Diehl, M. (2009). Robust nonlinear optimal control of dynamic systems with affine uncertainties. In *Proceedings of the 48th IEEE Conference on Decision and Control (CDC09)* (pp. 2274–2279). Shanghai (China).

Houska, B., Logist, F., Van Impe, J., & Diehl, M. (2012). Robust optimization of nonlinear dynamic systems with application to a jacketed tubular reactor. *Journal of Process Control*, *22*, 1152–1160.

Inselberg, A. (2009). *Parallel Coordinates*. Springer.

Jolliffe, I. (1986). *Principal Component Analysis*. Springer Verlag.

Julier, S. (2002). The scaled unscented transformation. In *Proceedings of the American Control Conference, 2002* (pp. 4555 – 4559). IEEE volume 6.

Julier, S., & Uhlmann, J. (1996). *A General Method for Approximating Nonlinear Transformations of Probability Distributions*. Technical Report Technical report, Robotics Research Group, Department of Engineering Science, University of Oxford.

Kohonen, T. (1998). The self-organizing map. *Neurocomputing*, *21*, 1–6.

Kollat, J. B., & Reed, P. (2007). A framework for visually interactive decision-making and design using evolutionary multi-objective optimization (video). *Environmental Modelling & Software*, *22*, 1691 – 1704.

Li, P., Arellano-Garcia, H., & Wozny, G. (2008). Chance constrained programming approach to process optimization under uncertainty. *Computers and Chemical Engineering*, *32*, 25 – 45.

Li, P., Wendt, M., & Wozny, G. (2002). A probabilistically constrained model predictive controller. *Automatica*, *38*, 1171 – 1176.

Logist, F., Houska, B., Diehl, M., & Van Impe, J. (2010). Fast pareto set generation for nonlinear optimal control problems with multiple objectives. *Structural and Multidisciplinary Optimization*, *42*, 591–603.

Journal homepage: http://www.journals.elsevier.com/expert-systems-with-applications
Original file available at: http://www.sciencedirect.com/science/article/pii/S0957417415003747

Postprint version of paper published in Expert Systems with Applications 2015, vol. 42, p. 7710-7731.
The content is identical to the published paper, but without the final typesetting by the publisher.

Logist, F., Houska, B., Diehl, M., & Van Impe, J. (2011). Robust multi-objective optimal control of uncertain (bio)chemical processes. *Chemical Engineering Science*, *66*, 4670 – 4682.

Logist, F., Vallerio, M., Houska, B., Diehl, M., & Van Impe, J. (2012). Multi-objective optimal control of chemical processes using ACADO toolkit. *Computers and Chemical Engineering*, *37*, 191–199.

Logist, F., & Van Impe, J. (2012a). Multi-objective dynamic optimisation of cyclic chemical reactors with distributed parameters. *Chemical Engineering Science*, *80*, 429–434.

Logist, F., & Van Impe, J. (2012b). Novel insights for multi-objective optimisation in engineering using normal boundary intersection and (enhanced) normalised normal constraint. *Structural and Multidisciplinary Optimization*, *45*, 417–431.

Luque, M., Lopez-Agudo, L., & Marcenaro-Gutierrez, O. (2015). Equivalent reference points in multiobjective programming. *Expert Systems with Applications*, *42*, 2205 – 2212.

Marler, R., & Arora, J. (2004). Survey of multi-objective optimization methods for engineering. *Structural and Multidisciplinary Optimization*, *26*, 369–395.

Mattson, C., & Messac, A. (2005). Pareto frontier based concept selection under uncertainty, with visualization. *Optimization and Engineering*, *6*, 85–115.

Messac, A., & Mattson, C. (2004). Normal constraint method with guarantee of even representation of complete Pareto frontier. *AIAA Journal*, *42*, 2101–2111.

Miettinen, K. (1999). *Nonlinear multiobjective optimization*. Boston: Kluwer Academic Publishers.

Miettinen, K., & Mäkelä, M. (1995). Interactive bundle-based method for non-differentiable multiobjeective optimization: NIMBUS. *Optimization*, *34*, 231–246.

Journal homepage: http://www.journals.elsevier.com/expert-systems-with-applications
Original file available at: http://www.sciencedirect.com/science/article/pii/S0957417415003747

Postprint version of paper published in Expert Systems with Applications 2015, vol. 42, p. 7710-7731.
The content is identical to the published paper, but without the final typesetting by the publisher.

Miller, G. A. (1956). The magical number seven, plus or minus two: some limits on our capacity for processing information. *Psychological review*, *63*, 81.

Mitra, K. (2009). Multiobjective optimization of an industrial grinding operation under uncertainty. *Chemical Engineering Science*, *64*, 5043–5056.

Montoya, F. G., Manzano-Agugliaro, F., Lapez-Marquez, S., Hernandez-Escobedo, Q., & Gil, C. (2014). Wind turbine selection for wind farm layout using multi-objective evolutionary algorithms. *Expert Systems with Applications*, *41*, 6585 – 6595.

Nagy, Z., & Braatz, R. (2004). Open-loop and closed-loop robust optimal control of batch processes using distributional and worst-case analysis. *Journal of Process Control*, *14*, 411–422.

Nagy, Z., & Braatz, R. (2007). Distributional uncertainty analysis using power series and polynomial chaos expansions. *Journal of Process Control*, *17*, 229 – 240.

Nagy, Z. K., & Braatz, R. D. (2003). Robust nonlinear model predictive control of batch processes. *AIChE Journal*, *49*, 1776 –1786.

Nikulin, Y., Miettinen, K., & Mäkelä, M. (2012). A new achievement scalarizing function based on parameterization in multiobjective optimization. *OR Spectrum*, *34*.

Ober-Blöbaum, S., & Seifried, A. (2013). A multiobjective optimization approach for optimal control problems of mechanical systems with uncertainties. In *Proceedings of the 13th European Control Conference (ECC)* (pp. 204 – 209).

Ojalehto, V., Podkopaev, D., & Miettinen, K. (2015). Agent assisted interactive algorithm for computationally demanding multiobjective optimization problems. *Computers and Chemical Engineering*, . doi:http://dx.doi.org/10.1016/j.compchemeng.2015.03.004.

Journal homepage: http://www.journals.elsevier.com/expert-systems-with-applications
Original file available at: http://www.sciencedirect.com/science/article/pii/S0957417415003747

Postprint version of paper published in Expert Systems with Applications 2015, vol. 42, p. 7710-7731.
The content is identical to the published paper, but without the final typesetting by the publisher.

Pascoletti, A., & Serafini, P. (1984). Scalarizing vector optimization problems. *Journal of Optimization Theory and Applications*, *42*, 499–524.

Pedro, L. R., & Takahashi, R. H. (2014). Inspm: An interactive evolutionary multi-objective algorithm with preference model. *Information Sciences*, *268*, 202 – 219.

Pontryagin, L., Boltyanskiy, V., Gamkrelidze, R., & Mishchenko, Y. (1962). *The mathematical theory of optimal processes*. New York: Wiley - Interscience.

Rahimi-Vahed, A., Rabbani, M., Tavakkoli-Moghaddam, R., Torabi, S., & Jolai, F. (2007). A multi-objective scatter search for a mixed-model assembly line sequencing problem. *Advanced Engineering Informatics*, *21*, 85 – 99.

Recker, S., Kühl, P., Diehl, M., & Bock, H. (2012). Sigmapoint approach for robust optimization of nonlinear dynamic systems. In *Proceeding of SIMULTECH 2012* (pp. 199–207).

Saaty, T., & Ozdemir, M. (2003). Why the magic number seven plus or minus two. *Mathematical and Computer Modelling*, *38*, 233 – 244.

Sahinidis, N. (2004). Optimization under uncertainty: state-of-the-art and opportunities. *Computers and Chemical Engineering*, *28*, 971–983.

Sanchis, J., Martinez, M., Blasco, X., & Salcedo, J. (2008). A new perspective on multiobjective optimization by enhanced normalized normal constraint method. *Structural and Multidisciplinary Optimization*, *36*, 537–546.

Sarkar, D., & Modak, J. (2004). Optimization of fed-batch bioreactors using genetic algorithm: multiple control variables. *Computers and Chemical Engineering*, *28*, 789–798.

Schenkendorf, R., Kremling, A., & Mangold, M. (2009). Optimal experimental design with the sigma point method. *Systems Biology, IET*, *3*, 10–23.

Sindhya, K., Ojalehto, V., Savolainen, J., Niemista, H., Hakanen, J., & Miettinen, K. (2014). Coupling dynamic simulation and interactive multiobjective

Journal homepage: http://www.journals.elsevier.com/expert-systems-with-applications
Original file available at: http://www.sciencedirect.com/science/article/pii/S0957417415003747

Postprint version of paper published in Expert Systems with Applications 2015, vol. 42, p. 7710-7731.
The content is identical to the published paper, but without the final typesetting by the publisher.

optimization for complex problems: An APROS-NIMBUS case study. *Expert Systems with Applications*, *41*, 2546 – 2558.

Sinha, A., Korhonen, P., Wallenius, J., & Deb, K. (2014). An interactive evolutionary multi-objective optimization algorithm with a limited number of decision maker calls. *European Journal of Operational Research*, *233*, 674 – 688.

Tarkkanen, S., Miettinen, K., Hakanen, J., & Isomäki, H. (2013). Incremental user-interface development for interactive multiobjective optimization. *Expert Systems with Applications*, *40*, 3220 – 3232.

Thomas, J. J., & Cook, K. (2005). *Illuminating the path: The research and development agenda for visual analytics*. IEEE Press.

Wächter, A., & Biegler, L. (2006). On the implementation of a primal-dual interior point filter line search algorithm for large-scale nonlinear programming. *Mathematical Programming*, *106*, 25–27.

Wendt, M., Li, P., & Wozny, G. (2002). Nonlinear chance-constrained process optimization under uncertainty. *Industrial and Engineering Chemistry Research*, *41*, 3621–3629.

Wierzbicki, A. P. (1980). The use of reference objectives in multiobjective optimization. In *Multiple Criteria Decision Making Theory and Application* (pp. 468–486). Springer Berlin Heidelberg volume 177 of *Lecture Notes in Economics and Mathematical Systems*.

Wierzbicki, A. P. (1982). A mathematical basis for satisficing decision making. *Mathematical Modelling*, *3*, 391 – 405. Special {IIASA} Issue.

You, F., Tao, L., Graziano, D. J., & Snyder, S. W. (2012). Optimal design of sustainable cellulosic biofuel supply chains: Multiobjective optimization coupled with life cycle assessment and input output analysis. *AIChE Journal*, *58*, 1157–1180.

Journal homepage: http://www.journals.elsevier.com/expert-systems-with-applications
Original file available at: http://www.sciencedirect.com/science/article/pii/S0957417415003747